ECMWF SEMINAR

6–9 September 2011

Data assimilation for atmosphere and ocean

The seminar will provide a pedagogical review of recent advances in data assimilation covering the topics:

Data assimilation methods

Particle filters and other non-linear data assimilation methods
Flow dependent background error in 4D-Var
Extended Kalman Filter surface analysis
Hybrid variational/ensemble methods
Long window weak constraint 4D-Var
Ensemble data assimilation

Observation related aspects

The global observing system
Assimilation of satellite data
Reanalysis
Pre and post processing
Observation error specification
Diagnostics of data assimilation

Real data assimilation systems

Hydrological cycle aspects
Stratospheric data assimilation
Mesoscale data assimilation
Ocean data assimilation
Coupled data assimilation: chemistry, aerosol, ocean, mixed layer

Efficient use of future computer architectures

For details of the programme see:
www.ecmwf.int/newsevents/seminars

Further information can be obtained from:
Els Kooij-Connally
ECMWF, Shinfield Park,
Reading, RG2 9AX, UK
E-mail els.kooij@ecmwf.int

ECMWF

Invited speakers

Sue Ballard *(University of Reading)*
Dale Barker *(Met Office)*
Massimo Bonavita *(ECMWF)*
Carla Cardinali *(ECMWF)*
Patricia De Rosnay *(ECMWF)*
John C. Derber *(NOAA/ NCEP)*
Gerald Desroziers *(Météo-France)*
Mike Fisher *(ECMWF)*
Keith Haines *(ESSC, University of Reading)*
Lars Isaksen *(ECMWF)*
Andrew Lorenc *(Met Office)*
Jean-François Mahfouf *(Météo-France)*
Andrew M Moore *(University of California)*
Saroja Polavarapu *(University of Toronto)*
Paul Poli *(ECMWF)*
Florence Rabier *(Météo-France)*
Michele Rienecker *(NASA-GMAO)*
Adrian Simmons *(ECMWF)*
Chris Snyder *(UCAR)*
Peter Jan van Leeuwen *(University of Reading)*
Jeffrey S. Whitaker *(NOAA ESRL)*

CONTENTS

PUBLICATION POLICY

The *ECMWF Newsletter* is published quarterly. Its purpose is to make users of ECMWF products, collaborators with ECMWF and the wider meteorological community aware of new developments at ECMWF and the use that can be made of ECMWF products. Most articles are prepared by staff at ECMWF, but articles are also welcome from people working elsewhere, especially those from Member States and Co-operating States. The *ECMWF Newsletter* is not peer-reviewed.

Editor: Bob Riddaway

Typesetting and Graphics: Rob Hine

Any queries about the content or distribution of the *ECMWF Newsletter* should be sent to Bob.Riddaway@ecmwf.int

Guidance about submitting an article is available at www.ecmwf.int/publications/newsletter/guidance.pdf

CONTACTING ECMWF

Shinfield Park, Reading, Berkshire RG2 9AX, UK

Fax: . . . . . +44 118 986 9450

Telephone: National 0118 949 9000

International . . . . . +44 118 949 9000

ECMWF website . . . . . http://www.ecmwf.int–

Front cover: Shows the averaged difference of the raw data measured by SMOS between the last and first week of April. It shows that larger SMOS brightness temperatures are observed over the UK at the end of April. Drier soil moisture conditions and larger vegetation water content both contribute to warmer SMOS brightness temperatures.

An ambitious future

When it was established in 1975, the challenge given to ECMWF was to develop medium-range weather forecasts to one week ahead. What appeared then as a dream is becoming a reality, with a typical range of good forecasts (anomaly correlation above 80%) reaching around 6 days. However this is clearly not the end of the story as new challenges are now presented to ECMWF. There is no doubt that the quality and range of forecasts can still be much increased and hence their applications will continue to grow.

Our first goal must be to further improve the forecast of severe weather across the medium-range, reaching a level of reliability that will allow mitigation action to be confidently implemented. Also improving the quality of the model will enhance the usefulness of forecasts of surface weather parameters such as precipitation, wind and temperature, which are certainly more directly usable than the 500 hPa geopotential height.

There are great expectations from society concerning better extended-range forecasts, namely monthly and seasonal forecasts. This is still very much research in progress, but recent successes in forecasting the last El Niño event one year in advance and last year's Russian heat wave several weeks ahead show that we are on the right track. The monthly forecasting system, which was launched less than 10 years ago as a test project, shows promising results and will open up new areas of application.

The development of ECMWF's numerical weather prediction systems has permitted its extension into new areas that will be of enormous benefit to society. The typical example is the capability to run reanalyses that have now proven to be a major tool for climate monitoring. Similarly, the possibility of including atmospheric chemistry in ECMWF's assimilation and forecasting systems will allow provision of air quality forecasts, the 'chemical weather forecast', in the same way as we have been accustomed to receiving weather forecasts. Another major application is the possibility of evaluating the impact of different observing systems, which is of course very beneficial given the huge costs of these systems.

In order to achieve these ambitious goals ECMWF will rely on the characteristics that served it well for more than 35 years:

- Remain focused on its area of expertise (i.e. global numerical weather prediction).
- Ensure the ability to attract the best European scientists and engineers, in particular offering them an efficient working environment and giving them challenging goals.
- Guarantee a strong interaction between research and operations.
- Federate potential across the Member States, in particular in the National Meteorological Services.
- Cooperate with the research community across Europe and worldwide.
- Complement and multiply the benefit of investments in Earth observations, in particular from satellites.

The scientific and technical aspects of the task ahead are more challenging than ever. Current times are also more difficult because of restrictions on public funding. Being a shared and jointly-funded European facility that delivers massive benefits to society will be a key element allowing ECMWF to continue the European success story started 35 years ago.

Dominique Marbouty

Changes to the operational forecasting system

DAVID RICHARDSON

New cycle (Cy37r2)

A new cycle of the ECMWF forecast and analysis system, Cy37r2, was implemented on 18 May. The new cycle includes both meteorological and technical changes. The main technical change is that from this cycle onwards the WMO FM-92 GRIB edition 2 (GRIB-2) will be used for the encoding of model-level data. The main meteorological changes included in this cycle are:

- Introduction of background error variances from the ensemble of data assimilations (EDA) used by the deterministic 4D-Var assimilation.
- Improvements to cloud scheme formulation.
- Reduction of AMSU-A observation errors and adjustments to MODIS Atmospheric Motion Vectors (AMVs).
- Changes to all-sky assimilation of microwave data.
- Accounting for tangent point drift in GPS radio occultation.

The impact of the new cycle on the performance of the forecasting system has been tested in research mode during the period June to December 2010, and in pre-operational runs during the period since 1 January 2011. The new cycle shows clear benefit in terms of objective upper-air scores in the medium range in both hemispheres: temperature and winds are improved throughout the troposphere. Tropical wind scores are also improved. The improvements to the cloud scheme increase the humidity in the upper troposphere. This results in some increase in bias, but overall provides a better fit to observations and improves humidity scores in the extra-tropics in the early forecast range.

There are no specific changes to the EPS configuration apart from the model changes described above. The impact on the EPS is a small reduction in spread throughout the forecast range. In terms of probabilistic scores the change is neutral.

Technical changes

From Cy37r2, ECMWF will use WMO FM-92 GRIB edition 2 (GRIB-2) encoding for its model-level fields for the deterministic forecast and the EPS, including monthly forecasts. GRIB-1 model-level data will no longer be produced and disseminated. This applies to model level products only; all other operational data will remain in GRIB-1.

More information on changes to the forecasting system can be found at:

- www.ecmwf.int/products/data/operational_system/evolution/

New items on the ECMWF website

ANDY BRADY

Survey on usage of the HPCF

ECMWF issued a short questionnaire to determine the level of user satisfaction with the HPCF service with the final goal to improve the service provided and help ECMWF to serve the users' needs better. The survey results and a full summary report are now available.

- http://www.ecmwf.int/services/computing/survey/hpcf-2010/

New cluster products

ECMWF has developed a new clustering application for the EPS. These products are now available operationally in dissemination, MARS and on the web. For the time being the new products will be provided in parallel to the old products. The new products are computed on a new European domain (domain=H). For type cluster means they will replace the old products and a new type cluster representative (type=CR) will be added. Type cluster standard deviations will not be produced.

- http://www.ecmwf.int/products/changes/clustering_2010/
- http://www.ecmwf.int/products/forecasts/d/charts/medium/eps/newclusters/

Joint ECMWF/ECOMET workshop for Catalogue Contact Points

This workshop was held at ECMWF on 4 and 5 April 2011. Topics included the rules, catalogue, tariffs and licensing arrangements for real-time products available from ECMWF or via ECOMET.

- http://www.ecmwf.int/newsevents/meetings/catalogue_contact_points/

Workshop on 'Representing model uncertainty and error in numerical weather and climate prediction models'

The workshop will be held at ECMWF from 20 to 24 June 2011. The workshop is co-sponsored by ECMWF, WMO/WGNE, WMO/THORPEX and WCRP. The purpose of this meeting is to (a) discuss the origins of model uncertainty in terms of physical processes, (b) compare the emerging methods for representing model uncertainty with the more 'traditional' methods, and (c) make recommendations on how this important area of model development should proceed.

- http://www.ecmwf.int/newsevents/meetings/workshops/2011/Model_uncertainty/

Annual Seminar on 'Data assimilation for atmosphere and ocean'

The seminar will give a pedagogical review of the principles behind data assimilation techniques and provide detailed descriptions of the currently used assimilation techniques. An overview of the observation data sources and their intrinsic properties

will be given. Outlooks on future developments in data assimilation such as ensemble based methods and weak constraint variational methods will also be included. Last but not least, challenges related to the design of efficient data assimilation schemes on future computer architectures will be addressed.

- http://www.ecmwf.int/newsevents/meetings/annual_seminar/2011/

Why aerosols matter: Advances in observations, modelling and understanding impacts

ECMWF will host a one meeting organized jointly by the Royal Meteorological Society and European Meteorological Society on 19 October 2011. The meeting will provide an overview of the latest advances in aerosol science and why aerosols matter. From dust storms to volcanic ash, forest fires to urban air pollution, clouds to climate change, the effects of aerosol are significant and widespread. The meeting will highlight the progress that has been made in observations, modelling and understanding the impacts of aerosol in our atmosphere.

- http://www.ecmwf.int/newsevents/meetings/hosted_meetings/RMS_2011/

13th Workshop on 'Meteorological Operational Systems'

The workshop will take place between 31 October and 4 November 2011. Objectives of the workshop have yet to be defined.

- http://www.ecmwf.int/newsevents/meetings/workshops/2011/MOS13/

ECMWF/GABLS Workshop on 'Diurnal cycles and the stable atmospheric boundary layer'

The ECMWF/GABLS Workshop will be held from 7 to 10 November 2011. The workshop will review the relevant research, consider the available schemes, explore the recent data sets and make recommendations for large scale models.

Since, the GEWEX Atmospheric Boundary Layer Studies Working Group (GABLS) has been addressing these issues for about 10 years, it is timely to review the results.

- http://www.ecmwf.int/newsevents/meetings/workshops/2011/GABLS/

Internal reorganisation within the Research and Operations Departments

ERLAND KÄLLÉN,
WALTER ZWIEFLHOFER

The internal organisation within the Research and Operations Departments at ECMWF was changed with effect from the 1 March 2011. The main purpose of the re-organisation is to adapt to gradual changes in the duties of the divisions and sections and also to create organisational structures that are ready to meet future challenges.

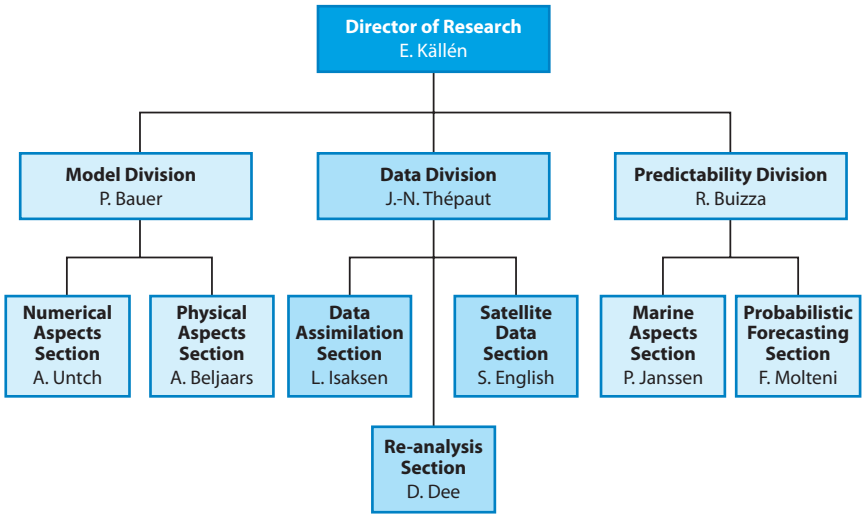

Changes in the Research Department

The Research Department at ECMWF originally started with two divisions: Model and Data Divisions. In 2002 a new division was created, the Probabilistic Forecasting and Diagnostics Division. The Seasonal Forecasting and Predictability Section and Diagnostics Section were moved into the new division and the pioneering work on ensemble forecasting systems for both the medium and extended ranges has been continued within the division. A research group working on ocean surface wave modelling evolved into a separate Ocean Waves Section and has been part of the Model Division since the late 1990s. Work on diagnostics was explicitly pursued within the Predictability and Diagnostics Section, but diagnostic methods have been developed and used within all sections of the Research Department.

The main purposes of this re-organisation within the Research Department are to:

- Merge the groups working on marine aspects (wave modelling and ocean modelling) into one section.
- Re-arrange the diagnostic activities such that they are more spread out within the divisions.

The reorganisation has affected the Probabilistic Forecasting and Diagnostics Division and Model Division, but the Data Division has been left unchanged. Overall the resulting Research Department structure has one section less than before while the size of the divisions remains about the same.

The Probabilistic Forecasting and Diagnostics Division has been renamed to simply the Predictability Division.

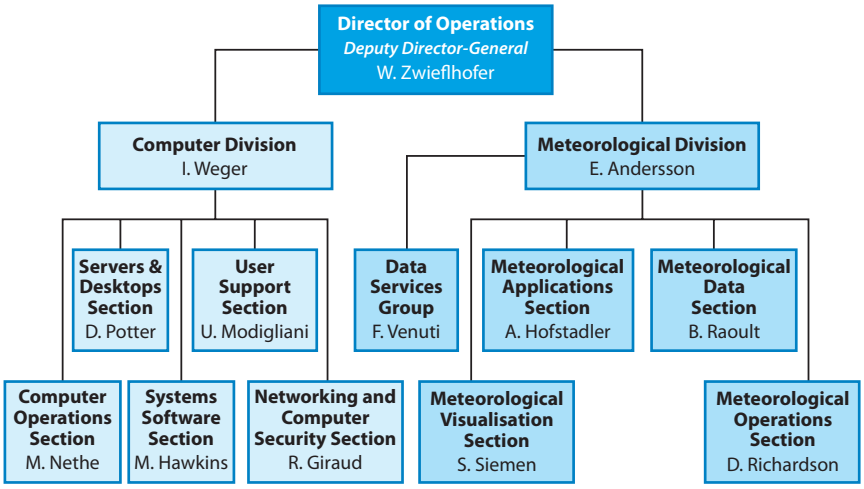

This is in line with the short names of the other two divisions. Two new sections have been formed in the division: Marine Aspects and Probabilistic Forecasting Sections.

Within the Model Division the following changes have been made. The Ocean Waves Section was moved to the Predictability Division and merged into the new section on Marine Aspects. Also two scientists have moved from the former Predictability and Diagnostics Section into the Physical Aspects Section.

In 2010 a Diagnostics Working Group was formed to intensify the across division/section and across departmental work on diagnostics. The group is chaired by a scientist in the Physical Aspects Section and in the new organisation each division has a full time scientist working on diagnostics. Also the Meteorological Operations Section in the Operations Department participates in the Diagnostics Working Group.

Changes in the Operations Department

The main purposes of the reorganisation in the Meteorological Division of the Operations Department are to:

- Strengthen the coordination of the Division's software development.
- Strengthen the position of the Data Services Team, taking into account that the responsibilities of the Meteorological Division are evolving.

The first goal is achieved by introducing the new role of Principal Software Architect. As the Centre's software and systems continue to grow in complexity, while the staff resources remain largely unchanged, it is essential to prevent duplication of efforts, reuse existing codes as much as possible and make use of available third-party software whenever that is appropriate.

The second goal is achieved by reassigning the duties within Data Services, with the newly-assigned Group Leader reporting directly to the Head of Division, and by strengthening the team with one additional consultant. The revenue generated by Data Services activity has become part of the Centre's general budget following Council's decision in December 2010. This in itself heightens the profile of this activity, increases the interactions with the Administration Department (Accounts and Legal/Contract Officer) and the importance of regular reporting.

The Data and Services Section has been renamed the Meteorological Data Section and the Graphics Section has been renamed the Meteorological Visualisation Section. The role of 'Principal Software Architect' has been assigned to the current Head of the Meteorological Data Section.

At the same time, the teams behind the MARS and product generation software development have been strengthened. The responsibilities of the Meteorological Visualisation Section now include ecCharts (the new web-based forecasters' tool), maintenance of interpolation software and EMOSLIB. The expected benefits are better integration and coordination of this software with tools such as Magics and Metview.

The Computer Division has been left unchanged.

New modular building

UTE DAHREMÖLLER

The installation of a new two-storey modular building on the site of the former 'Terrapin Towers' is nearing completion.

The building offers some 390 m² of temporary accommodation including offices for 20 people, a small meeting room, kitchen, photocopy room and toilets on both floors.

We have worked very closely with our consultants and the contractor, Modular UK, to produce a design which offers enhanced structural rigidity and acoustic and thermal properties combined with a contemporary appearance. Consequently the new 'North Building' provides an adequate working environment for the people located there.

The new North Building was ready for occupation at the end of May 2011.

New Member States

MANFRED KLÖPPEL

Accession agreements have been signed which will lead to Iceland and Slovenia becoming ECMWF Member States. As full Member States, they will acquire full voting rights at the ECMWF Council from the date of the enforcement of the agreement. Also a portion of the Centre's computer and archive resources will be allocated to them for their own use.

The original Convention restricted ECMWF's membership to the founding Member States. Amendments to the Convention entered into force on 6 June 2010, allowing more States to accede to the Convention.

Agreement with Iceland

On 9 March 2011, Mrs Svandís Svavarsdóttir, Minister for the Environment of Iceland, and Mr Dominique Marbouty, Director-General of ECMWF, signed an accession agreement in Reykjavik. Mr Árni Snorrason, Director-General of the Icelandic Meteorological Office, attended the ceremony.

Mrs Svandís Svavarsdóttir stated: "It is an honour for me to sign the accession agreement with the ECMWF, one of the world's leading centres in numerical weather prediction. This is a major milestone for Iceland in establishing closer links to European centres of excellence, such as ECMWF. I would like to express my appreciation of the ECMWF Council voting unanimously in favour of Iceland's accession to the ECMWF Convention on 24 February 2011."

Mr Árni Snorrason said: "Since Iceland became a Co-operating State in December 1980, the Icelandic Meteorological Office has been able to make good use of ECMWF's products, in particular to improve our forecasts. Above all, the Centre's forecasts of extreme weather events are vital to enable us to prepare for and respond to those events. I am looking forward to even closer collaboration with our colleagues at ECMWF."

Mrs Svandís Svavarsdóttir, Minister for the Environment of Iceland, and Mr Dominique Marbouty, Director-General of ECMWF, signing the accession agreement in Reykjavik on 9 March 2011.

Agreement with Slovenia

On 8 April 2011, Mr Roko Žarnić, Slovenian Minister for Environment and Spatial Planning, and Mr Dominique Marbouty, Director-General of ECMWF, signed an assession agreement in Ljubljana. Mr Silvo Žlebir, Director General of Slovenian Environment Agency, and Mr Klemen Bergant, Director of Slovenian Meteorological Office and Permanent Representative of Slovenia with WMO, also attended the ceremony.

Minister Roko Žarnić stated: "I would like to thank the ECMWF Council for having unanimously adopted the Resolution on the accession of Slovenia to the ECMWF Convention on 31 March 2011. It is an honour for me to sign the accession agreement with ECMWF. This is an important milestone for Slovenia. Establishing closer links to European centres of excellence, such as ECMWF, is one of the key strategic goals of the government of the Republic of Slovenia."

Mr Silvo Žlebir said: "ECMWF is the world's leading centre in global medium-range weather prediction. Since Slovenia became a Co-operating State in 1997, the Slovenian Meteorological Office has been able to make good use of ECMWF's data and products, which helped to significantly improve our forecasts. The Centre's forecasts of extreme weather events, such as wind storms and heavy precipitation, are vital to enable us to prepare for and respond to those events."

Mr Klemen Bergant added: "The benefits of using ECMWF products for early warnings were clearly evident in recent extreme weather events such as the strong Bora winds in March 2010 and March 2011, as well as the floods in December 2009 and September 2010. Based on ECMWF products, early warnings were issued to the Slovenian Administration for Civil Protection and Disaster Relief as well as to the public. Civil protection units were well prepared and the public was informed about the threat in advance. Therefore, material damage was reduced and lives were saved despite the severity of these events."

Mr Roko Žarnić, Slovenian Minister for Environment and Spatial Planning, and Mr Dominique Marbouty, Director-General of ECMWF, signing the accession agreement in Ljubljana on 8 April 2011.

New clustering products

LAURA FERRANTI, SUSANNA CORTI

THE ECMWF clustering is one of a range of products that summarise the large amount of information in the Ensemble Prediction System (EPS). The clustering gives an overview of the different synoptic flow patterns in the EPS. Based on the similarity between their 500 hPa geopotential fields over the North Atlantic and Europe, the members are grouped together.

EPS cluster products have been produced operationally since 1992. In recent years, due to the continuous improvements of the EPS (in particular reduced spread, consistent with decreasing ensemble mean error), these products only occasionally produced more than one cluster. The requirement for cluster products was recently reviewed with ECMWF's Member and Co-operating States, particularly during the annual Forecast Products Users' Meeting. Although some countries do their own clustering (for specific parameters or areas of interest), there was a clear requirement for ECMWF to continue providing a general cluster product from the EPS. Therefore, based on the feedback from the Member and Co-operating States, a new EPS clustering application was developed. The new clustering was endorsed by the TAC Subgroup on Verification Measures as part of their review of product development and user requirements.

The new system includes two components:

- A daily clustering of the forecast fields from the EPS, similar in principle to the original EPS clustering but using a different algorithm.
- A set of four fixed climatological regimes.

The daily clustering summarises the range of synoptic flow patterns in the current EPS. Each cluster is represented by the EPS member closest to its centre, referred to as the 'EPS scenario' for that cluster. Each EPS scenario is then attributed to one of the four climatological regimes. This shows the differences between scenarios in terms of the large-scale flow and provides information about the possible transitions between regimes during the forecast. This approach also enables the development of flow-dependent skill measures.

The new cluster products were implemented operationally in November 2010. This article describes the new clustering, introduces the new cluster products and provides information on how to use them. Validation of the new clustering is also addressed.

The new EPS clustering

The clustering algorithm takes the 51 forecasts (50 perturbed plus 1 control forecast) and groups together those that show a similar evolution of the 500 hPa geopotential over the North Atlantic and Europe (75°N–30°N, 20°W–40°E). For two EPS members to join the same cluster they must display similar synoptic development at 500 hPa throughout a given time window. Clustering in this way, rather than on individual forecast days, has the advantage that temporal continuity and synoptic consistency are retained. The clustering is made independently for four time windows: 72–96, 120–168, 192–240 and 264–360 hour forecast ranges.

The number of clusters can vary from case to case. In some cases the EPS will contain a number of well-separated groups of similar forecasts (a so called multimodal distribution). In other cases the EPS members will be rather more evenly spread out, with no clear grouping into separate clusters (a so called unimodal distribution): there is in effect just a single cluster containing all ensemble members. Since the clustering is intended as a summary of the ensemble information, the maximum number of clusters is limited; the maximum is six as in the previous clustering.

Details of the procedure to compute the clusters are given in the Appendix.

Large-scale climatological regimes

To put the daily clustering in the context of the large-scale flow and to allow the investigation of regime changes, the new ECMWF clustering contains a second component. Each cluster is attributed to one of a set of four pre-defined climatological regimes:

- Positive phase of the North Atlantic Oscillation (NAO).
- Euro-Atlantic blocking.
- Negative phase of the North Atlantic Oscillation (NAO).
- Atlantic ridge.

The climatological regimes have been computed from 29 years of reanalysis data (ERA-Interim and ERA-40) using the same clustering algorithm as for the EPS scenarios (see the Appendix). They are consistent with those documented in the literature (see, for example, *Michelangeli et al.*, 1995).

Figure 1 shows the climatological regimes computed for the cold season (October to April). The climatological regimes for the warm season (May to September) have very similar patterns, but with lower amplitude. To account for this seasonal evolution, in the classification of the EPS scenarios the patterns and amplitudes of the climatological regimes are adjusted month by month. A pattern-matching algorithm assigns each EPS scenario to the closest climatological weather regime (in terms of the root mean square difference).

Using the new cluster products

The new cluster products are archived in MARS and available to forecast users through the operational dissemination of products. A graphical product using the new clustering is available for registered users on the ECMWF web site:

- http://www.ecmwf.int/products/forecasts/d/guide/medium/eps/newclusters/.

This web product is designed to provide forecasters with an overview of the EPS clusters for the current forecast.

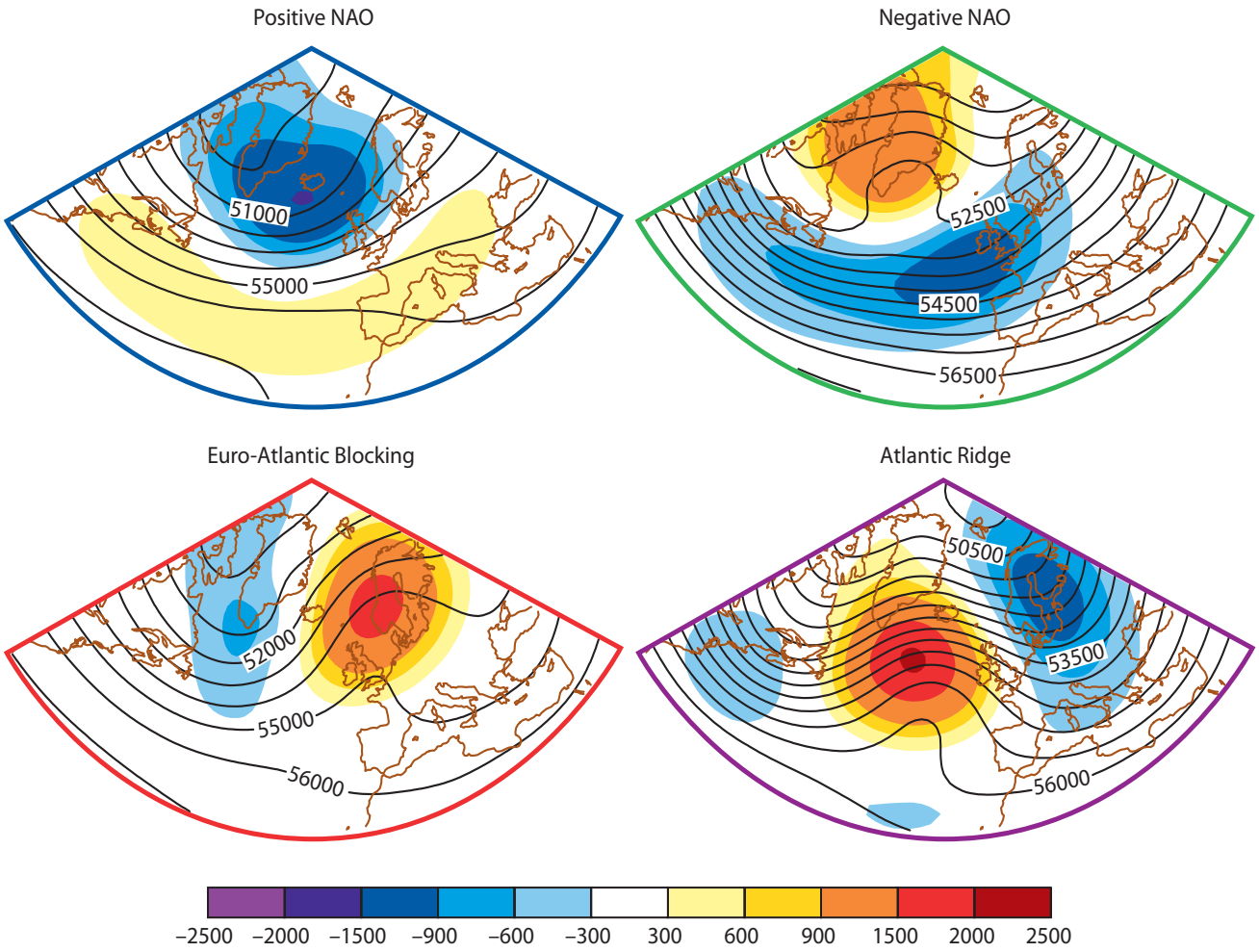

Figure 1 Geographical patterns of the four Euro-Atlantic climatological regimes (both anomalies and full fields) associated with the cold season climatological regimes computed as clusters in the phase-space spanned by the ten leading empirical orthogonal functions (EOFs). The geopotential anomalies (colour shading) and geopotential (contours) at 500 hPa are shown. The corresponding patterns for the warm season are available at http://www.ecmwf.int/products/forecasts/cluster_doc/era_cl4_mjjas_1980-2008.gif

An example is shown in Figure 2 for the 120–168 hour (5–7 day) time window for the forecast from 00 UTC on 2 February 2011. There are three clusters with each cluster represented by one of its members: the forecast closest to the centre of the cluster. The representative members of the three clusters are referred to as the 'EPS scenarios'. These three EPS scenarios are shown at the beginning (120 hours, left column), middle (144 hours, centre) and end (168 hours, right) of the forecast time window. The top row shows the EPS scenario for the first cluster: there are 22 members in this cluster and the control forecast (labelled member 0) has been identified as the representative member of that cluster. The second row shows the EPS scenario for the second cluster: member 29, representing the 15 members of this cluster; member 46, the EPS scenario for the 14 members of cluster 3 is shown in the bottom row.

Users need to be careful in interpreting the number of clusters. There is no direct link between the number of clusters and the overall spread of the ensemble. For example, the EPS may contain a large range of solutions (large spread) but without forming distinct clusters. Alternatively there may be several distinct solutions, but all within the same general flow type (so small overall spread). Because the clustering is done separately for each time window, it is quite possible to have more clusters at the short range that at longer range.

The second component of the new clustering, the four fixed climatological weather regimes, is able to provide additional information. Each EPS scenario is attributed to one of the four climatological regimes. This attribution is shown in Figure 2 by the coloured border round each panel; the colours match those of the corresponding regime shown in Figure 1.

The synoptic forecast evolutions shown in Figure 2 can now be seen in the context the underlying large-scale pattern in which the synoptic features of the weather scenarios are embedded. To help with this interpretation, the panels in Figure 2 show both the forecast geopotential and the anomaly (the difference between the forecast and the climatological 500 hPa geopotential fields). At the beginning of the time window (120 hours into the forecast, left panels) all three scenarios are in the positive NAO regime (all have blue frames). 48 hours later (right panels), each EPS scenario has evolved towards a different large-scale flow regime.

- Scenario 1 (top panel), showing reinforced westerly flow crossing the Atlantic, is related to the positive NAO regime.

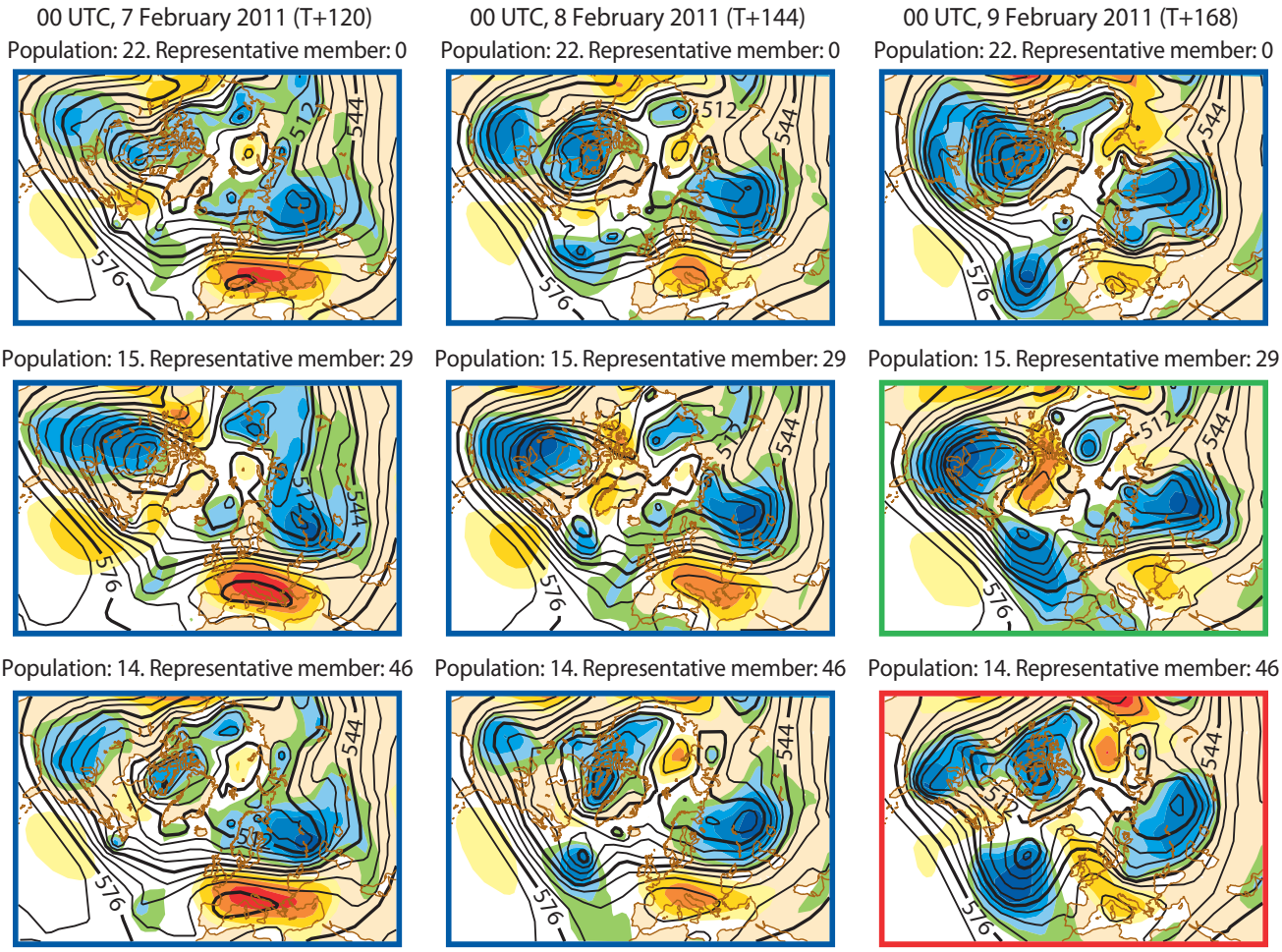

Figure 2 EPS scenarios for time window 120–168 hours for the forecast initiated 2 February 2011. Maps of geopotential at 500 hPa and anomalies from a 29-year reanalysis climate (colour shading: red positive, blue negative). The geopotential field is scaled by 100.

- Scenario 2 (middle panel), with a deeper low over the Azores and a further reduction of westerlies, exhibits the typical negative NAO circulation pattern.
- Scenario 3 (bottom panel), with an anticyclonic circulation penetrating UK, is consistent with the main features of the Euro-Atlantic blocking.

Since all members are equally likely, the number of members in each EPS cluster provides an indication of the scenario probability (see Box A). Cluster 1 (22 members) has the highest probability, while cluster 2 (15 members) and cluster 3 (14 members) are equally likely. The additional information from the climatological regimes shows that there is a growing uncertainty through the forecast in the large-scale flow pattern. By day 7 (168 hours into the forecast), although the most likely cluster (cluster 1) remains in the positive NAO regime, both the other clusters indicate a change in the large-scale flow. There is some uncertainty about which regime transition will occur, but it is more likely than not that the overall characteristics of the large-scale flow will change.

The web site includes the products equivalent to Figure 2 for each of the four time windows. For additional information, the 1000 hPa geopotential fields are also provided for each EPS scenario to show the corresponding near-surface evolution. The user should bear in mind that the clustering has been made on the 500 hPa fields; if the main focus of the user is the surface fields we suggest the users compute the clusters using surface parameters.

Use of the climatological regimes in validating the EPS performance

The classification of each EPS scenario in terms of pre-defined climatological regimes provides an objective measure of the differences between scenarios in terms of large-scale flow patterns. This attribution enables flow-dependent verification and a more systematic analysis of EPS performance in predicting regimes transitions.

An example of the use of the climatological regimes in validating the EPS performance is given in Figure 3. For the period September to November 2010, this shows the number of EPS scenarios forecast each day (bars) and their classification (colour coded) with respect to the climatological regimes. The time window is 120–168 hours and the classification is made for the EPS scenarios at forecast range 168 hours. The sequence of coloured circles represents the 'observed' climatological regimes computed from the verifying analysis.

Figure 3 shows three distinct blocking events (red circles), each persisting for about a week (second week of September, beginning of October and late November), two periods with a persistent Atlantic ridge flow pattern (violet, mid

Objective validation of the performance of the new products

A

An objective validation of the performance of the new products has been developed. Such evaluation will be routinely updated, including a larger amount of forecast data as it becomes available. The Continuous Ranked Probability Scores (CRPS) evaluates the performance of the EPS as a probabilistic forecast; it is negatively oriented so smaller values indicate better forecast performance. The CRPS computed for a deterministic forecast is the same as the mean absolute error.

The figure compares the CRPS of the probabilistic forecast based on the full 51-member EPS distribution with the CRPS using probabilities derived from the number of members in each EPS cluster (this is referred to as the 'scenario distribution'). Also shown are the CRPS values for five reduced size ensembles with a maximum of six members and for the ensemble mean.

The scenario distribution is constructed by assuming that each scenario represents perfectly all the other members belonging to that cluster. Consider a case with three clusters with populations of 11, 22 and 18 members. The scenario distribution is then computed taking 11 times scenario 1, 22 times scenario 2 and 18 times scenario 3. The additional reduced size ensembles are constructed by extracting each day a number of random members equal to the number of clusters obtained for that day.

The performance of the scenario distribution is significantly better than that of any random reduced size ensembles. This indicates that the cluster scenarios are better at representing the whole EPS distribution. The results for the ensemble mean, being undistinguishable from the reduced ensemble with six members, indicates that a randomly chosen ensemble with maximum ensemble size of six has a CRPS equivalent to that of the ensemble mean. This implies that an EPS with a maximum of six randomly chosen members does not provide more information in a probabilistic sense than a deterministic forecast represented by the average of 51 members.

It is important to mention that the probabilistic scores depend largely on the ensemble size. The smaller the ensemble size, the more sensitive are the scores. For ensembles larger than 20–25 members the probabilistic scores start to be less responsive to the ensemble size. A large ensemble provides a more detailed and more reliable estimate of the forecast distribution. So it is not surprising that the full EPS provides a better probabilistic forecast than using just the scenarios. However the clustering products represent a compromise between the advantages of condensing forecast information using a few EPS scenarios against the disadvantage of losing information associated with the full 51 EPS members. The difference in CRPS between the whole EPS distribution and the CRPS of the scenario distribution reminds the users of the extent of such a compromise.

Similar skill estimates to those shown in the figure, but calculated by considering only cases when a selected climatological regime is observed, have also been calculated. The results from this flow-dependent verification are not shown here since currently the amount of data is not considered sufficient for a robust analysis. However, such verification results could be of great value to the users during the formulation of their forecast.

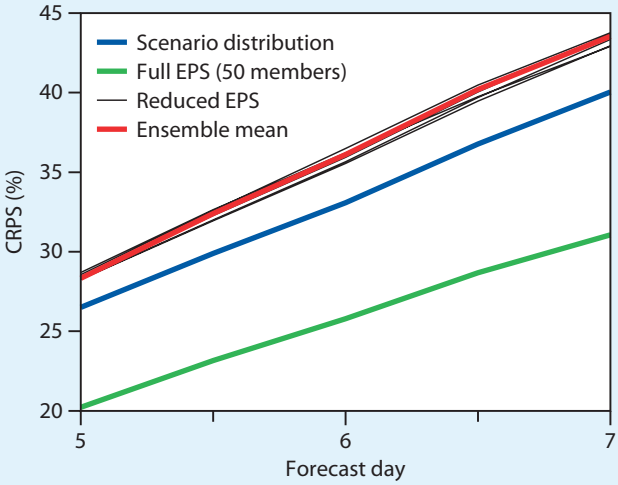

CRPS for the EPS as represented by the scenario distribution, the full 51 member EPS distribution, the five reduced EPS ensembles and ensemble mean. The period considered is January to November 2010.

September and second half of October) one of which extends up to two weeks, and a number of shorter-term regimes transitions.

During the two weeks of the persistent Atlantic ridge regime (13–26 October) the number of EPS scenarios ranges between 2 and 5, showing that the number of distinct synoptic evolutions within the EPS varies from day to day. However, throughout this period, all but two of the scenarios are attributed to the same Atlantic ridge regime. So the EPS is giving a strong signal that this is a period of enhanced large-scale predictability and transition to a different regime is unlikely. The beginning and end of this persistent period were both well forecast by the EPS. After four days in the blocking regime (7–10 October), over the next two days the EPS showed increasing probability of the change to the Atlantic ridge regime. At the end of October, the breakdown of this regime was also clearly signalled. Unlike the previous transition, the EPS indicated considerable uncertainty about what large-scale would follow this breakdown, and indeed in terms of the large-scale flow the end of October and beginning of November was rather changeable.

This verification shows that, as a general feature, cases where the EPS scenarios are associated with different

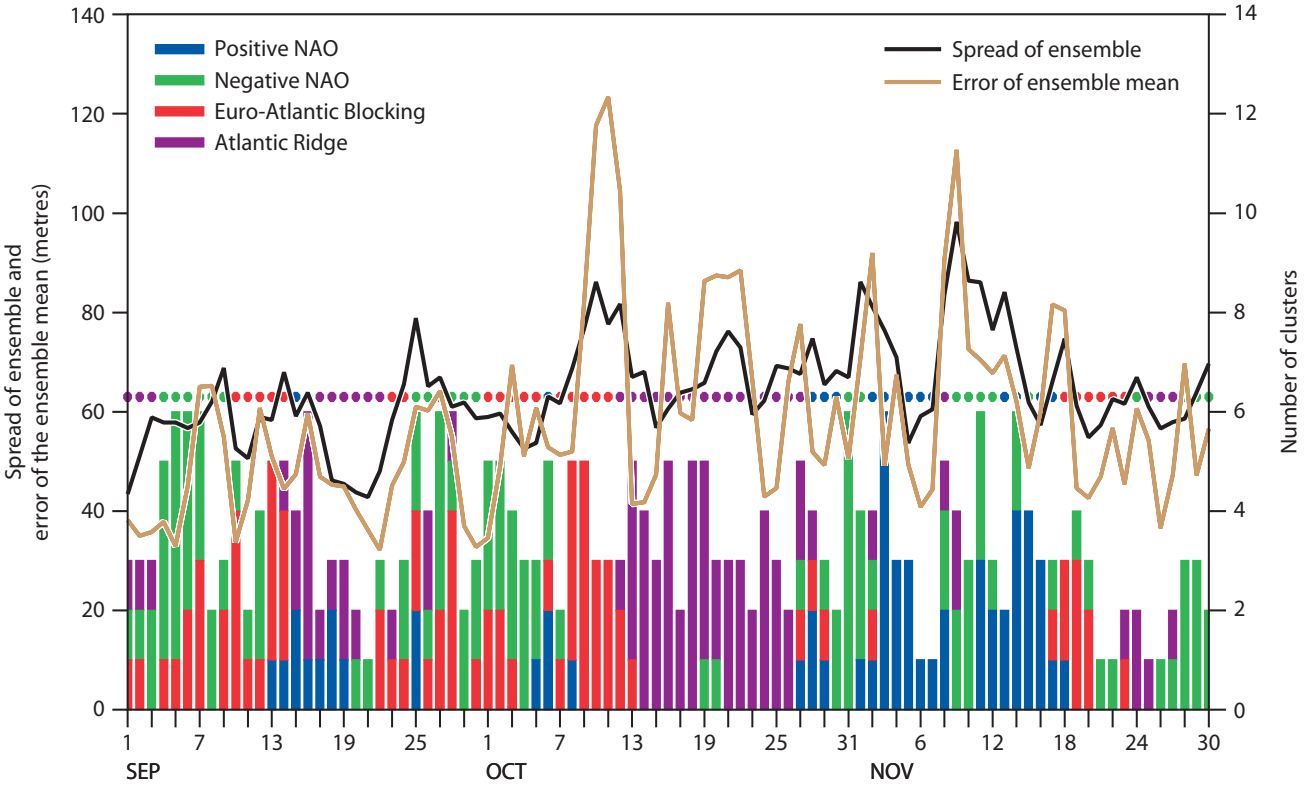

Figure 3 Daily time series for September to November 2010 of the number of EPS scenarios (the colours refer to the patterns shown in Figure 1), spread of the ensemble, error of the ensemble mean, and observed climatological regimes (coloured circles).

climatological regimes (bars have several colours) occur at periods when regimes transitions take place. Conversely, the periods with a persistent observed regime are associated with a reduced level of forecast 'large-scale diversity' and consequently an enhanced level of predictability. Overall during the autumn 2010 season the EPS scenarios successfully captured the observed time evolution of the climatological regimes.

Figure 3 also shows the ensemble spread (ensemble standard deviation) and error of the ensemble mean forecast for each case. It is worth noting that the mean of both quantities over the season are comparable. This indicates that the EPS is well constructed and the verifying analysis will generally lie within the range of solutions predicted by the ensemble. However, as discussed in the previous section, Figure 3 shows that the cases with high spread do not always correspond to forecasts with a large number of scenarios.

Summary and future developments

After consultation with ECMWF's Member and Co-operating States, ECMWF has developed a new clustering application for the EPS. The new clustering extends the current clustering by providing additional information about the forecast in terms of large-scale climatological regimes. This gives the potential to prediction transitions between regimes and allows the development of flow-dependent verification of the EPS.

A new web product has been developed. This shows the EPS scenarios (the members representing each cluster) and also indicates the climatological regime associated with each scenario. Thus users are provided with a summary of the range of synoptic developments in the current EPS forecast and complementary information about the likelihood of transitions between climatological regimes. Initial validation results show that the EPS can predict these regime transitions. More objective verification of the regime transitions and of the flow-dependent behaviour of the EPS will be developed.

ECMWF will investigate extending the new clustering to cover the full time range of the monthly forecast, considering for example time windows of 2 to 4 weeks ahead. The new clustering methodology can also be adapted to produce additional products appropriate to the needs of individual users (e.g. different domains, variables and forecast ranges); the software could be implemented locally in Member States. In future it may be possible to provide the clustering as a flexible tool via a web interface to allow the user to make such tailored products.

Appendix. Methodology for identifying EPS scenarios and climatological regimes

The cluster algorithm used to identify both EPS scenarios and climatological regimes is based on the modified K-means method applied in *Straus et al.* (2007). This methodology can be summarized in the following four steps.

Identification of a suitable phase space for the cluster computation. Clustering techniques are effective only if applied in an L-dimensional phase space with $L<N$, where N is the number of elements in the dataset (for the EPS, N=51, the number of members in the ensemble). Because

the North Atlantic and Europe area contains many more than 51 grid points, it is first necessary to transform the forecasts to a new much lower dimensional co-ordinate system. This is done using so-called empirical orthogonal functions (EOFs). The clustering is carried out in the reduced phase space defined by the L leading EOFs that explain at least 80% of the total variance of the dataset. The associated principal components (PCs) provide the new coordinates. For the EPS, the clusters are computed in an extended time window (e.g. the 120–168 hour forecast range), so EOFs extended in time are used.

Computation of the optimal partition of the data. For a given number k, the optimum partition of the data into k clusters is found. k members are allocated as (pseudorandom) 'seed points'. An initial clustering is then made based on the distance from these seeds. The algorithm takes this initial cluster assignment and iteratively changes it by assigning each element to the cluster with the closest centroid, until a 'stable' classification is achieved. (A cluster centroid is defined by the average of the PC coordinates of all states that lie in that cluster.)

This process is repeated many times (using different seeds), and for each partition the ratio r^*_k of the variance among cluster centroids (weighted by the cluster population) to the average intra-cluster variance is recorded. The optimal partition is the one that maximises this ratio.

Assessment of the significance of a given k-partition. The goal is to assess the strength of the clustering compared to that expected from an appropriate reference distribution, such as a multi-dimensional Gaussian distribution. In assessing whether the null hypothesis of multi-normality can be rejected, it is necessary to perform Monte-Carlo simulations using a large number M of synthetic data sets. Each synthetic data set has precisely the same size (number of members) as the original data set against which it is compared. They are generated from a series of L dimensional Markov processes whose mean, variance and first-order auto-correlation are obtained from the observed data set. A cluster analysis is performed for each one of the simulated data sets. For each k-partition the ratio r_{mk} of variance among cluster centroids to the average intra-cluster variance is recorded.

Since the synthetic data are assumed to have a unimodal distribution, the proportion P_k of synthetic samples for which $r_{mk} < r^*_k$ is a measure of the significance of the k-cluster partition of the actual data, and $1–P_k$ is the corresponding confidence level for the existence of k clusters.

Choice of the most suitable number of clusters. The need to specify the number of clusters can be a disadvantage of the K-means method if we do not know in advance how many clusters to expect. However, there are three main criteria that can be used to choose the optimal number of clusters: (i) *Significance*: the partition with the highest significance (P_k) with respect to predefined multi-normal distributions (see previous step); (ii) *Reproducibility*: we can use as a measure of reproducibility the ratio of the mean-squared error of best matching cluster centroids from N pairs of randomly chosen half-length data sets from the full original data set. The partition with the best reproducibility (ratio closest to one) will be chosen; (iii) *Consistency*: this can be calculated both with respect to the choice of variable (for example comparing with clusters obtained from different dynamically linked variables) and with respect to the specified domain (test of sensitivities to changing the horizontal or vertical domain).

All three criteria have been used to identify the most suitable number of climatological regimes.

However, for the daily clustering only the statistical significance test is used; due to the limited sample size (51 ensemble members), reproducibility and consistency cannot be properly estimated. The number of clusters is determined as follows.

- If the significance (P_k) of all considered cluster partitions, from 2 to 6 clusters, is below a minimum threshold of 55%, it is assumed that there are no clusters.
- If the minimum significance threshold is achieved, then the partition with the highest significance is chosen.
- If more than one partition has a significance value higher than 95%, the one with the minimum number of clusters is chosen.

An additional criterion is used to evaluate the EPS cluster partition, based on the ratio between the average internal variance of clusters and the mean EPS variance of the season. For each time window all the partitions in which the average internal variance of the clusters is lower than 50% of the mean EPS variance are discarded. This condition limits the occurrence of large numbers of clusters (five or six) and, by taking into consideration that the ensemble spread is a function of forecast range, it adds some consistency in the cluster population between the four forecast time ranges.

However, due to well known features of the K-means methodology (*Michelangeli et al.*, 1995), there can still be too many cases with the maximum number of EPS clusters (here this is set to six). To avoid this, if the six cluster partition is selected and its significance is at least 93%, a check is made for other cluster partitions that have 90% or higher significance: the partition with the fewest clusters that satisfies this significance level is chosen instead of the six cluster partition.

FURTHER READING

Michelangeli, P.-A., R. Vautard & B. Legras, 1995: Weather regimes: Recurrences and quasi-stationarity. *J. Atmos. Sci.*, **52**, 1237–1256.

Straus, D., M.S. Corti & F. Molteni, 2007: Circulation regimes: chaotic variability versus SST-forced predictability. *J. Climate*, **20**, 2251–2272.

Extended Kalman Filter soil-moisture analysis in the IFS

PATRICIA DE ROSNAY, MATTHIAS DRUSCH, GIANPAOLO BALSAMO, CLÉMENT ALBERGEL, LARS ISAKSEN

A NEW soil moisture analysis scheme based on a point-wise Extended Kalman Filter (EKF) was implemented at ECMWF with cycle 36r4 of the Integrated Forecasting System (IFS) in November 2010. The EKF soil moisture analysis replaces the previous Optimum Interpolation (OI) scheme, which was used in operations from July 1999 (IFS cycle 21r2) to November 2010. In continuity with the previous system it uses 2-metre air temperature and relative humidity observations to analyse soil moisture. The computing cost of the EKF soil moisture analysis is significantly higher than that of the OI scheme. So, as part of the EKF soil moisture analysis implementation, a new surface analysis structure was implemented in September 2009 (cycle 35r3) to move the surface analysis out of the time critical path.

The main justifications for implementing the EKF soil moisture analysis are as follows.

- In contrast to the OI scheme, which uses fixed calibrated coefficients to describe the relationship between an observation and model soil moisture, the EKF soil moisture increments result from dynamical estimates that quantify accurately the physical relationship between an observation and soil moisture.
- The EKF scheme is flexible to cope with the current increase in model complexity. In particular, changes in the IFS and in the land-surface model H-TESSEL (Hydrology Tiled ECMWF Scheme for Surface Exchanges over Land) are accounted for in the analysis increments computation.
- The EKF soil moisture analysis makes it possible to use soil moisture data from satellites and to combine different sources of information (i.e. active and passive microwave satellite data, and conventional observations).
- It considers the observation and model errors during the analysis in a statistically optimal way and allows assimilation of observations at their correct observation times.

The implementation and evaluation of the EKF soil moisture analysis is described in this article. An overview is given of a set of one-year analysis experiments conducted to assess the performance of the EKF. These experiments led to the implementation of the EKF in November 2010 using screen-level parameters to analyse soil moisture. The impact of ASCAT (Advanced SCATterometer) data assimilation is also briefly presented to investigate the possibility to combine conventional observations and satellite data for the soil moisture analysis.

Sources of data

The ECMWF operational soil moisture analysis system is based on analysed screen-level variables (2-metre temperature and relative humidity). In the absence of a near-real time global network for providing soil moisture information, using screen-level data is the only source of information that has been continuously available for NWP soil moisture analysis systems. It provides indirect, but relevant information to analyse soil moisture.

In the past few years several new space-borne microwave sensors have been developed that measure soil moisture. They provide spatially integrated information on surface soil moisture at a scale relevant for NWP models.

- The active sensor ASCAT on MetOp was launched in 2006. The EUMETSAT ASCAT surface soil moisture product is the first operational soil moisture product. It is available in near-real time on EUMETCAST and it has been monitored operationally at ECMWF since September 2009.
- ESA's SMOS (Soil Moisture and Ocean Salinity) mission was launched in 2009. Based on L-band passive microwave measurements, SMOS is the first mission dedicated to providing information about soil moisture.
- The future NASA SMAP (Soil Moisture Active and Passive) mission, planed to be launched in 2015, will be a soil moisture mission that combines active and passive microwave measurements to provide global soil moisture and freeze/thaw state.

ECMWF plays a major role in developing and investigating the use of new satellite data for soil moisture analysis. For example, the EUMETSAT ASCAT soil moisture product has been monitored operationally at ECMWF since September 2009 and SMOS brightness temperature product has been monitored in near-real time since November 2010:

- http://www.ecmwf.int/products/forecasts/d/charts/monitoring/satellite/slmoist/ascat/
- http://nwmstest.ecmwf.int/products/forecasts/d/charts/monitoring/satellite/smos

Implementation of SMOS data monitoring at ECMWF is described in an accompanying paper by *Muñoz Sabater et al.* in this edition of the *ECMWF Newsletter* (pages 23–27).

The ECMWF land-surface analysis system

The ECMWF land-surface analysis includes the analysis of snow depth, screen-level parameters (2-metre temperature and relative humidity) as well as soil moisture and soil temperature. It is performed independently from the 4D-Var atmospheric analysis. The upper-air analysis and the land-surface analysis are used together as initial conditions for the forecast. In turn, the model-predicted fields provide the first guess and initial conditions of the next land-surface and upper-air analysis cycle.

So, surface analysis indirectly interacts with the upper-air analysis of the next cycle through its influence on the forecast that propagates information from one cycle to the next.

The surface analysis is performed at fixed times at 0000, 0600, 1200, and 1800 UTC. With the re-structured surface analysis it is able to run at the same time as the two main 12-hour windows used in the 4D-Var atmospheric analyses; these cover the periods from 2100 to 0900 UTC and from 0900 to 2100 UTC.

The soil moisture analysis is based on the analysis of screen-level parameters which provides gridded information on 2-metre temperature and relative humidity. So, screen-level SYNOP data is used as proxy information for the soil moisture analysis, based on the relationship between soil variables (moisture and temperature) and the near-surface atmosphere controlled by evaporation processes.

With the OI soil moisture analysis, soil wetness and 2-metre temperature (relative humidity) increments were assumed to be negatively (positively) correlated.Therefore the 2-metre analysis increments of temperature and relative humidity were used as input for the soil moisture OI scheme as described in *Mahfouf* (2000). Soil moisture analysis increments were computed analytically for each model grid point for the four soil moisture layers of the land-surface model H-TESSEL. The OI soil moisture analysis scheme improved the boundary layer forecasts skill, but not soil moisture in which errors were allowed to accumulate, as shown in *Drusch et al.* (2008).

In order to improve the use of conventional observations and enable use of land-surface satellite measurements, an advanced surface data assimilation system, based on an Extended Kalman Filter (EKF) approach, was developed by *Drusch et al.* (2008). With this approach, the EKF coefficients are dynamically estimated, so the soil moisture corrections account for meteorological forcing (radiative and precipitation) and soil moisture conditions. There is also the possibility of simultaneously assimilating screen-level observations and satellite data such as ASCAT surface soil moisture or SMOS brightness temperature products. The EKF soil moisture analysis is a point wise data assimilation scheme – the scheme used at ECMWF is outlined in Box A.

EKF Soil Moisture Analysis implementation

Although the OI system is limited in terms of both performances and flexibility in its use of different types of data, the OI system has the great advantage of being very cheap in computing time. At any resolutions the OI time consumption remains negligible, ranging from about 3 seconds in CPU at T159 (125 km) to 20 seconds in CPU at T799 (25 km).

The EKF surface analysis is far more expensive than the OI system. At T159 its time consumption is close to 3×10^3 seconds in CPU. At T255 it increases to 10^4 CPU seconds and it is close to 2×10^5 CPU seconds at T799, for which is represents about one fifth of the 4D-Var time consumption. It was implemented to be used at T1279 in operations where it uses the same number of processors and threads as the upper-air analysis, leading to an elapsed time of 750 seconds (7×10^5 CPU seconds).

EKF soil-moisture analysis scheme **A**

For each grid point, the analysed soil moisture state vector $\boldsymbol{\theta}_a$ is computed as:

$$\boldsymbol{\theta}_a = \boldsymbol{\theta}_b + \boldsymbol{K}(\boldsymbol{y}-\boldsymbol{H}\,\boldsymbol{\theta}_b)$$

with $\boldsymbol{\theta}_b$ the background soil moisture state vector, $\boldsymbol{H}$ the Jacobian matrix of the observation operator, $\boldsymbol{y}$ the observation vector and $\boldsymbol{K}$ the Kalman gain matrix which accounts for the Jacobian matrix, and the covariance matrix of background and observation errors. In this system the observation vector can include:

- Conventional observations such as 2-metre temperature and relative humidity.
- Satellite measurements of soil moisture (e.g. ASCAT product) or any other measurement related to soil moisture (e.g. SMOS, brightness temperatures).

The elements of the Jacobian matrix used in the analysis scheme are estimated in finite differences by perturbing individually each analysed soil layer. In contrast to the OI scheme, the EKF Jacobians are computed for each soil layer to account for the soil water diffusion processes. Therefore computed soil moisture increments for each grid point of the model follow a vertical profile that results from a physically-based estimate of the relationship between the soil moisture profile and the parameters in the lower atmospheric level.

In order to enable the implementation of the EKF soil moisture analysis, the surface analysis structure was first revised in IFS cycle 35r3. In previous cycles the surface analysis was performed after the upper-air analysis. The surface analysis got observations from the upper-air analysis observations data base and some of the surface analysis input fields (10-metre wind components and albedo) were outputs from the upper-air analysis. Hence, the surface analysis had to wait for the upper-air analysis to be completed and there were some dependencies between the 4D-Var and the surface analysis. As a consequence the surface analysis was performed in the time critical path.

A new structure of the surface analysis was implemented with IFS cycle 35r3 in September 2009, with the surface analysis now being independent of the upper-air analysis. The observational dependency was resolved by creating a new observation data base dedicated to surface analysis. Consequently the field dependency issue mentioned above is resolved by using the first-guess fields instead of the upper-air analysis output fields. This means that the new surface analysis and the upper-air analysis are separated, so, they can be run in parallel. So, the surface analysis is not in the critical path anymore, thereby opening up the possibility of using a more sophisticated surface analysis scheme.

The new surface analysis structure constitutes an essential step in the ongoing developments of the surface analysis in the IFS. By removing the surface analysis tasks from the time critical path, it enabled the implementation of the EKF soil moisture analysis in IFS cycle 36r4 in November 2010.

Tests of the EKF soil moisture analysis

Experimental set up

In preparation for implementing the EKF soil moisture analysis three analysis experiments were conducted at T255 resolution over a one-year period (December 2008 to 30 November 2009).

- ***'OI' experiment***. The OI soil moisture analysis uses the increments of the screen-level parameters analysis as input. It represents the operational soil moisture analysis configuration that was used in operations at ECMWF from July 1999 to November 2010.
- ***'EKF' experiment***. This uses the dynamical EKF soil moisture analysis, in which the analysis of screen-level parameters is used as proxy information for soil moisture.
- ***'EKF+ASCAT' experiment***. This was conducted for the same one-year period using the EKF in which the analysis of screen-level parameters is used together with the ASCAT soil moisture data.

In this 'EKF+ASCAT' experiment, ASCAT soil moisture data is matched to the ECMWF IFS model soil moisture using a Cumulative Distribution Function (CDF) matching as described in *Scipal et al.* (2008). A first demonstration of the impact of using a nudging scheme has already been performed by *Scipal et al.* (2008). They showed, however, that compared to the OI system, using scatterometer data slightly degraded the forecast scores. They recommended using ASCAT data in an EKF analysis to account for observation errors and to combine ASCAT data with screen-level proxy information. This is investigated in the 'EKF+ASCAT' experiment.

Note that:

- The 'OI' and 'EKF' experiments only differ in the method used for the soil moisture analysis. Observations used for the analysis are identical.
- The 'EKF' and 'EKF+ASCAT' experiments use the same EKF scheme, but satellite data is used in addition to conventional data in the 'EKF+ASCAT' experiment.

One month of spin-up is considered for the first month of the experiment, so results presented here focus on the period January to November 2009.

Comparing the 'OI' and 'EKF' experiments

Figure 1 shows monthly accumulated soil moisture increments for the first metre of soil for July 2009 for the OI and EKF experiments, and their difference . Spatial patterns of soil moisture increments are quite similar for the OI and EKF schemes. For both the OI and the EKF the soil moisture increments are generally positive in most areas. However, negative increments are found in Argentina, Alaska and North East of America. These results mainly show that the EKF soil moisture analysis generally reduces the soil moisture analysis increments compared to the OI scheme.

Figure 2 shows the annual cycle of the global mean soil moisture increments for the OI and EKF experiments. It can be seen that the soil moisture increments of the OI scheme systematically add water to the soil. The global monthly mean value of the OI analysis increments is 5.5 mm, which represents a substantial and unrealistic contribution to the global water

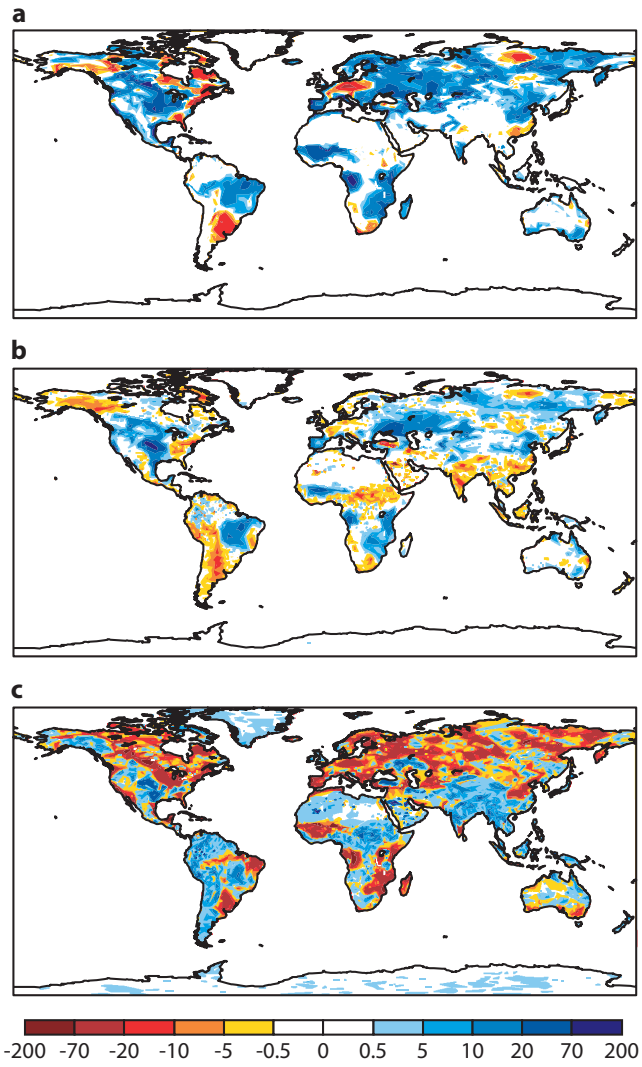

Figure 1 Monthly soil moisture increments (mm) within the top soil metre root zone (in mm) during July 2009 produced by (a) OI scheme and (b) EKF scheme. (c) Difference between EKF and OI schemes.

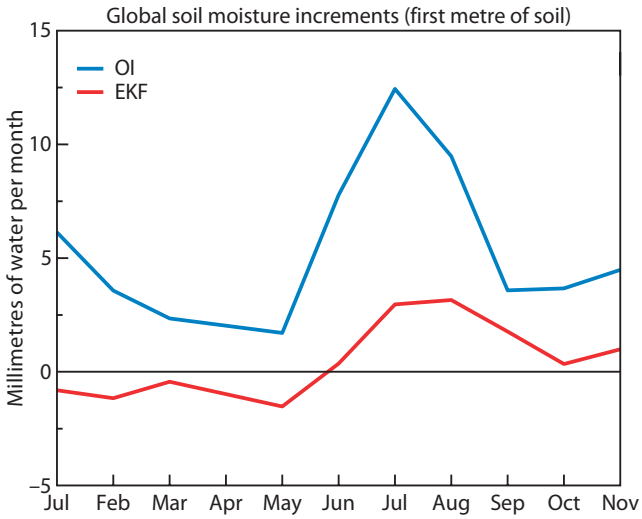

Figure 2 Temporal evolution of soil moisture increments in the first metre of soil (global mean value) in mm of water per month from January to November 2009, produced by the OI and EKF schemes.

cycle. In contrast the EKF global mean soil moisture analysis increments are much smaller, representing global monthly mean increments of 0.5 mm. The reduction of increments between the EKF and the OI is mainly due to the reduction in increments below the first layer. The OI increments computed for the first layer are amplified for deeper layers in proportion to the layer thickness, explaining the overestimation of OI increments. In contrast the EKF dynamical estimates, based on perturbed simulations, allow the optimizing of soil moisture increments at different depths to match screen-level observations according to the strength of the local and current soil-vegetation-atmosphere coupling. The EKF accounts for additional controls due to meteorological forcing and soil moisture conditions. Thereby it prevents undesirable and excessive soil moisture corrections.

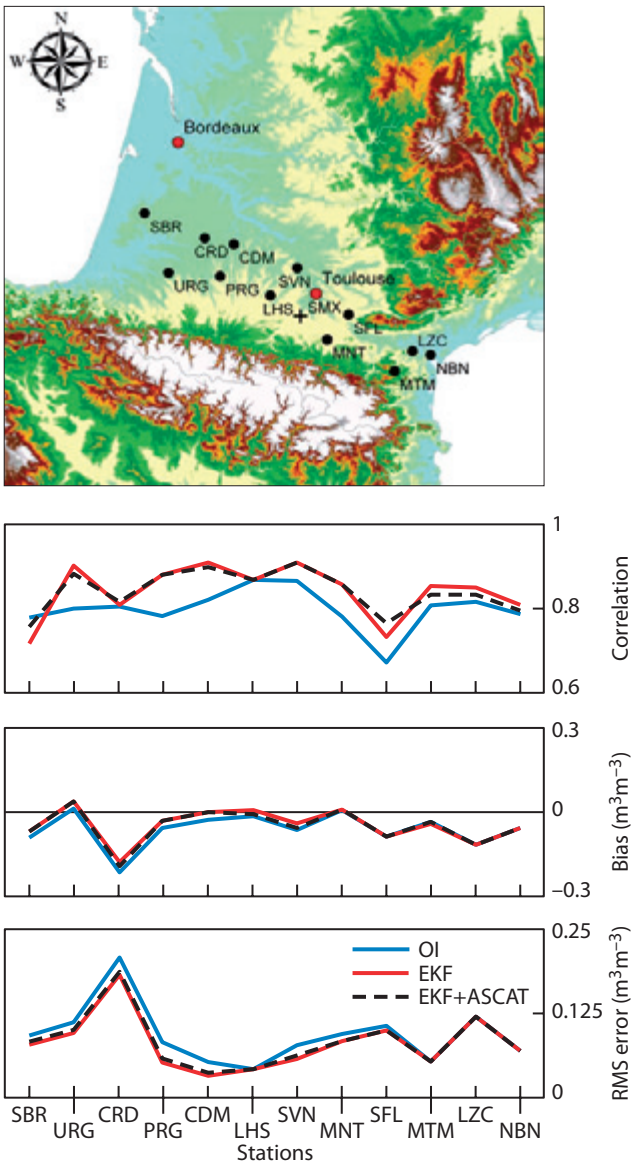

Figure 3 Correlation, bias (observation minus model) and root-mean-square (RMS) error of ECMWF surface soil moisture analysis of layer 1 for the 12 soil moisture stations in the SMOSMANIA (soil moisture observing system – meteorological automatic network integrated application) network in Southwest France in 2009, for the OI, EKF and EFF+ASCAT configurations of the soil moisture analysis.

Comparing 'OI', 'EKF' and EKF+ASCAT' experiments

Figure 3 shows the impact of the soil moisture analysis scheme on analysed soil moisture of the first soil layer (0–7cm) for all three experiments. Evaluation is conducted for 2009 against the 12 SMOSMANIA ground stations of the operational soil moisture network of Météo-France (*Calvet et al.*, 2007). It shows that ECMWF soil moisture is generally in good agreement with ground observations, with mean correlations higher than 0.78.

Using the EKF instead of the OI scheme improves significantly the soil moisture analysis, leading to a remarkable agreement between ECMWF soil moisture and ground truth (mean correlation higher than 0.84 for EKF and EKF+ASCAT). The bias and root-mean-square error are also improved with the EKF compared to the OI scheme. One may note that a strong negative bias is indicated for all schemes for one station, indicating that the analysis overestimates soil moisture content. This systematic difference in terms of volumetric soil moisture content is related to soil texture issues in this area for which the local ground data is not representative of the ECMWF model soil texture.

Results obtained from the EKF+ASCAT experiment show that using ASCAT does not improve the performance of the soil moisture analysis. In the experiment where ASCAT data is assimilated, soil moisture data has been re-scaled to the model soil moisture using a CDF matching, as described in *Scipal et al.* (2008). The matching corrects observation bias and variance. So, in the data assimilation scheme only the observed ASCAT soil moisture variability is assimilated.

In Figure 3, the impact of ASCAT data assimilation might be limited by both the quality of the current ASCAT product and the CDF-matching approach used in the assimilation scheme. EUMETSAT recently revised the processing of the ASCAT soil moisture product to reduce the ASCAT product noise level. Test conducted with the new product prototype (not shown) considerably improved the usage of the ASCAT soil moisture data. Future experiments using an improved CDF-matching, with H-TESSEL corrected from precipitation errors, and improved data quality are expected to improve the impact of using ASCAT soil moisture in the data assimilation.

Impact on first guess and forecasts

Figure 4 shows the global impact of the EKF on the 2-metre temperature first guess that enters the analysis. The EKF soil moisture analysis scheme slightly improves the 2-metre temperature scores by consistently reducing the bias of the first-guess.

Figure 5 is an evaluation of the 48-hour forecast of 2-metre temperature (at 0000 UTC) for the African continent. It shows that the EKF reduces the night time cold bias compared to the OI scheme. Also the specific humidity (not shown) generally indicates drier conditions with the EKF than the OI scheme. Note that the ASCAT soil moisture data does not impact on screen-level variables and it has only a slight impact on soil moisture analysis as shown in Figure 3.

Figure 6 shows the monthly mean impact of the EKF soil moisture analysis on the 48-hour forecast of 2-metre

temperature at 0000 UTC for July 2009. It indicates the difference in temperature error (in K) between the OI and EKF experiments. Positive values indicate that the EKF generally improves the 2-metre temperature forecasts compared to the OI soil moisture analysis. In most areas the 2-metre temperature errors for OI are larger than the EKF errors, showing that the EKF soil moisture analysis has a positive impact on the 2-metre temperature forecast.

Summary and future developments

An Extended Kalman Filter (EKF) soil moisture analysis was implemented in operations with IFS cycle 36r4 in November 2010. Compared to the previous OI scheme, the EKF is a dynamical scheme that accounts for non-linear control on the soil moisture increments (meteorological forcing and soil moisture conditions). So, it prevents undesirable and excessive soil moisture corrections, and reduces the soil moisture analysis increments. This significantly improves the performance of the soil moisture analysis, as verified against independent soil moisture observations. The new analysis scheme has a moderate impact on the atmospheric scores although it slightly improves the 2-metre temperature by reducing the cold bias in Europe and Africa.

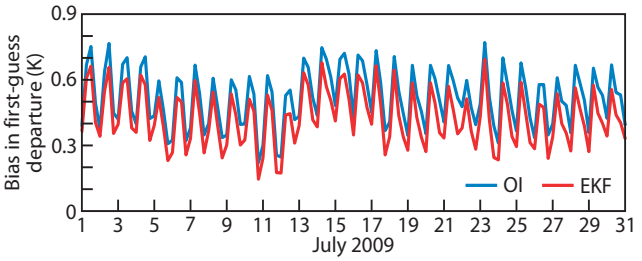

Figure 4 Temporal evolution of the bias in the first-guess departure (global mean) of the 2-metre temperature in July 2009 obtained wih the OI and EKF soil moisture analyses.

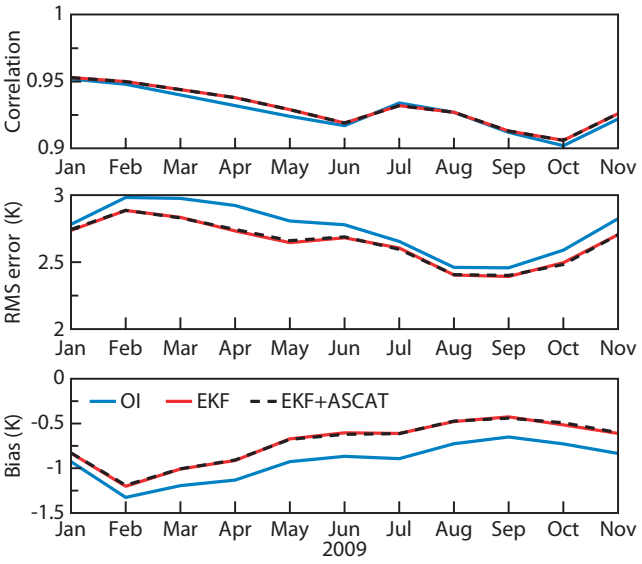

Figure 5 Correlation, root-mean-square (RMS) error and bias of 2-metre temperatures against SYNOP data in Africa from January 2009 to November 2009 for the OI and EKF schemes as implemented in operations (i.e. using conventional data of screen-level temperature and humidity), and the EKF when conventional data is combined with satellite soil moisture data from ASCAT.

The EKF soil moisture analysis enables the combined use of screen-level parameters and satellite data, such as ASCAT soil moisture data, to analyse soil moisture. Results with ASCAT data assimilation show a neutral impact on both soil moisture and screen-level parameters. However improvements in the ASCAT soil moisture products and in bias correction are expected to improve the impact of using ASCAT soil moisture data.

The new EKF soil moisture analysis system opens a wide range of further development possibilities, including exploiting new satellite surface data and products for the assimilation of soil moisture. An extension of the EKF to analyse additional variables, such as snow mass and vegetation parameters, is planned for investigation in the near future.

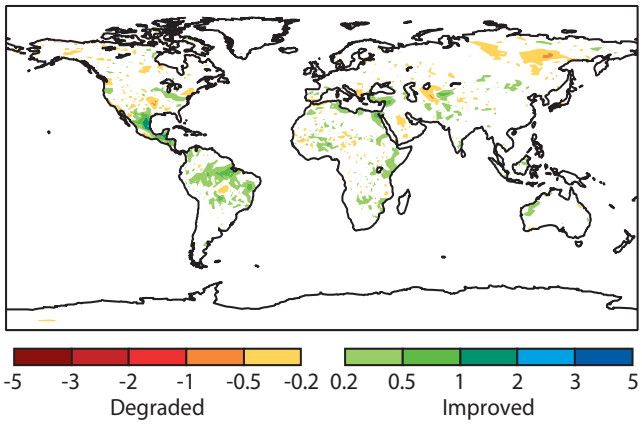

Figure 6 Monthly mean difference for July 2009 between the errors in the 36-hour forecasts (12 UTC) of 2-metre temperature for the OI and the EKF soil moisture analysis schemes. The forecasts are verified against the operational analysis.

FURTHER READING

Calvet, **J.-C.**, **N. Fritz**, **F. Froissard**, **D. Suquia**, **A. Petitpa** & **B. Piguet**, 2007: In situ soil moisture observations for the CAL/VAL of SMOS: the SMOSMANIA network. *International Geoscience and Remote Sensing Symposium*, IGARSS, Barcelona, Spain, doi: 10.1109/IGARSS.2007.4423019, 2007.

de Rosnay, **P.**, **M. Drusch**, **G. Balsamo**, **A. Beljaars**, **L. Isaksen**, **D. Vasiljevic**, **C. Albergel** & **K. Scipal**, 2009: Advances in land data assimilation at ECMWF. In *Proc. ECMWF/GLASS Workshop on Land Surface*, Reading, UK, 9–12 November 2009, http://www.ecmwf.int/publications/library/do/references/show?id=89853

Drusch, **M.**, **K. Scipal**, **P. de Rosnay**, **G. Balsamo**, **E. Andersson**, **P. Bougeault** & **P. Viterbo**, 2008: Exploitation of satellite data in the surface analysis. *ECMWF Tech. Memo. No. 576*, http://www.ecmwf.int/publications/library/do/references/show?id=88712

Mahfouf, **J.-F.**, 2000: A revised land-surface analysis scheme in the Intergrated Forecasting System. *ECMWF Newsletter No. 88*, 8–13, http://www.ecmwf.int/publications/newsletters/pdf/88.pdf

Scipal, **K.**, **M. Drusch** & **W. Wagner**, 2008: Assimilation of a ERS scatterometer derived soil moisture index in the ECMWF numerical weather prediction system. *Adv. Water Res.*, doi:10.1016/j.advwatres.2008.04013.

Evolution of land-surface processes in the IFS

GIANPAOLO BALSAMO, SOUHAIL BOUSSETTA, EMANUEL DUTRA, ANTON BELJAARS, PEDRO VITERBO, BART VAN DEN HURK

MAJOR UPGRADES have been implemented over the last few years in the soil hydrology, snow and vegetation components of the ECMWF land-surface parametrization. Compared to the scheme used in ERA-Interim and ERA-40 reanalyses, the current model has an improved match to soil moisture and snow field-site observations with a beneficial impact on the forecasts of surface energy and water fluxes and near-surface temperature and humidity. This is verified by conventional synoptic observations and by dedicated flux-tower sites for forecasts ranging from daily to seasonal. The gain in hydrological consistency is also of crucial importance for data assimilation of land-surface satellite observations in water sensitive channels. The scheme described here, currently used for daily medium-range forecasts, will be adopted by the new Seasonal Forecasting System and included in future reanalyses.

A brief description of the main hydrological components of the land-surface model with selected validation results will now be presented followed by an outlook for future research activities.

Development of the land-surface model

In recent years the land-surface modelling at ECMWF has been extensively revised. An improved soil hydrology (*Balsamo et al.*, 2009), a new snow scheme (*Dutra et al.*, 2010) and a multi-year satellite-based vegetation climatology (*Boussetta et al.*, 2011) have been included in the operational Integrated Forecasting System (IFS). These have had a positive impact on both the global hydrological water cycle and near-surface temperatures compared to the TESSEL (Tiled ECMWF Scheme for Surface Exchanges over Land) scheme which was used in the ECMWF's ERA-40 and ERA-Interim reanalyses.

In particular the soil hydrology affected the quality of seasonal predictions during extreme events associated with soil moisture-precipitation feedback as in the European summer heat-wave in 2003 (*Weisheimer et al.*, 2011). The new snow scheme improved the thermal energy exchange at the surface with a substantial reduction of near-surface temperature errors in snow-dominated areas (i.e. northern territories of Eurasia and Canada).

More recently, the introduction of a monthly climatology for vegetation Leaf Area Index (LAI) to replace the fixed maximum LAI has shown a reduction of near-surface temperature errors in the tropical and mid-latitude areas, particularly evident in spring and summer. At the same time the bare ground evaporation has been enhanced over deserts by adopting a lower stress threshold than for vegetation. This is in agreement with experimental findings (e.g. *Mahfouf & Noilhan*, 1991) and results in a more realistic soil moisture for dry-lands.

The participation in international projects such as GLACE2 (Global Land-Atmosphere Coupling Experiment-2) and AMMA (African Monsoon Multidisciplinary Analysis), in which the ECMWF model was coupled with a realistic set of soil moisture fields, have improved the understanding of the mechanisms and areas of strong coupling between the land surface and the atmosphere.

The land-surface components

TESSEL as documented by van den *Hurk et al.* (2000) and *Viterbo & Beljaars* (1995) is the backbone of the current operational land-surface scheme at ECMWF. It includes up to six land-surface tiles (bare ground, low and high vegetation, intercepted water, and shaded and exposed snow) which can co-exist under the same atmospheric grid-box. Recent revisions of the soil and snow hydrology as well as vegetation characteristics are illustrated in Figure 1.

Soil hydrology

A revised soil hydrology in TESSEL was investigated by van den *Hurk & Viterbo* (2003) for the Baltic basin. These model developments were a response to known weaknesses of the TESSEL hydrology: specifically the choice of a single global soil texture, which does not characterize different soil moisture regimes, and an infiltration-excess runoff scheme which produces hardly any surface runoff. Therefore, a revised formulation of the soil hydrological conductivity and diffusivity (spatially variable according to a global soil texture map) and surface runoff (based on the variable infiltration capacity approach) were introduced in IFS Cy32r3 in November 2007. *Balsamo et al.* (2009) verified the impact of HTESSEL from field site to global atmospheric coupled experiments and in data assimilation.

Snow hydrology

A fully revised snow scheme has been introduced in 2009 to improve the existing scheme based on *Douville et al.* (1995). The snow density formulation was changed and a liquid water storage in the snow-pack was introduced, which also allows the interception of rainfall. On the radiative side, the snow albedo and the snow cover fraction have been revised and the forest albedo in presence of snow has been retuned based on MODIS satellite estimates. A detailed description of the new snow scheme and a verification from field site experiments to global offline simulations is presented in *Dutra et al.* (2010). The results showed an improved evolution of the simulated snow-pack with positive effects on the timing of runoff and terrestrial water storage variation and a better match of the albedo to satellite products.

TESSEL (June 2000)

Van den Hurk et al. (2000)
Viterbo & Beljaars (1995), *Viterbo et al.* (1999)
- Up to 8 tiles (binary Land-Sea mask)
- GLCC vegetation (BATS-like)
- ERA-40 and ERA-Interim scheme

Land surface tiles in ERA-40/ERA-Interim surface scheme

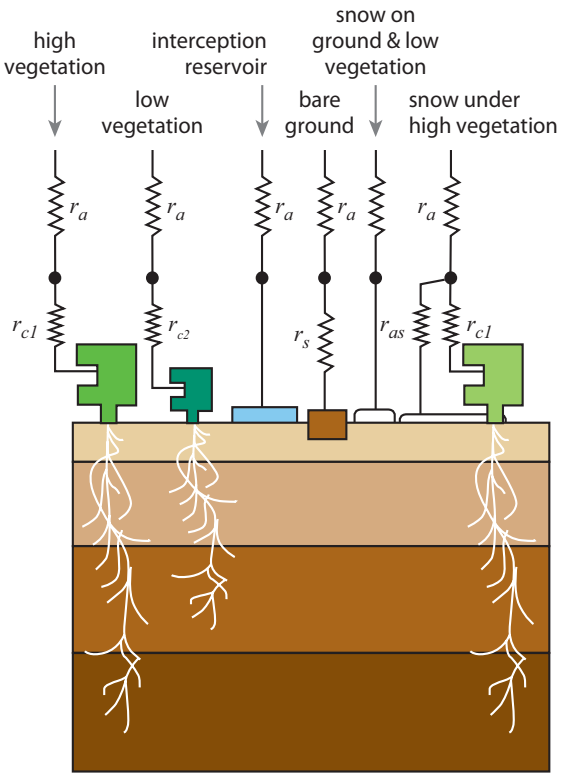

New snow (March and September 2009)

Dutra et al. (2010)
- Revised snow density
- Liquid water reservoir
- Revision of albedo and sub-grid snow cover

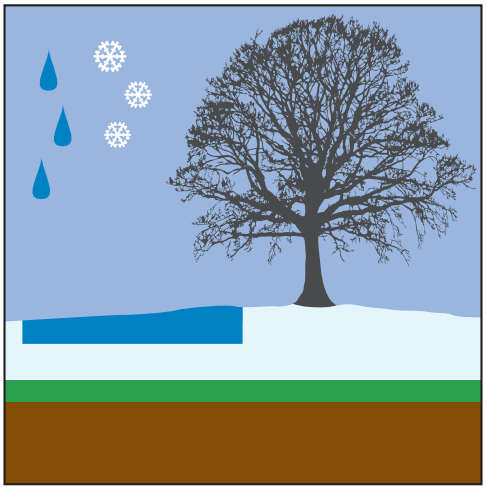

Hydrology TESSEL (November 2007)

Balsamo et al. (2009)
van den Hurk & Viterbo (2003)
- Global Soil Texture (FAO)
- New hydraulic properties
- Variable infiltration capacity and surface run-off revision

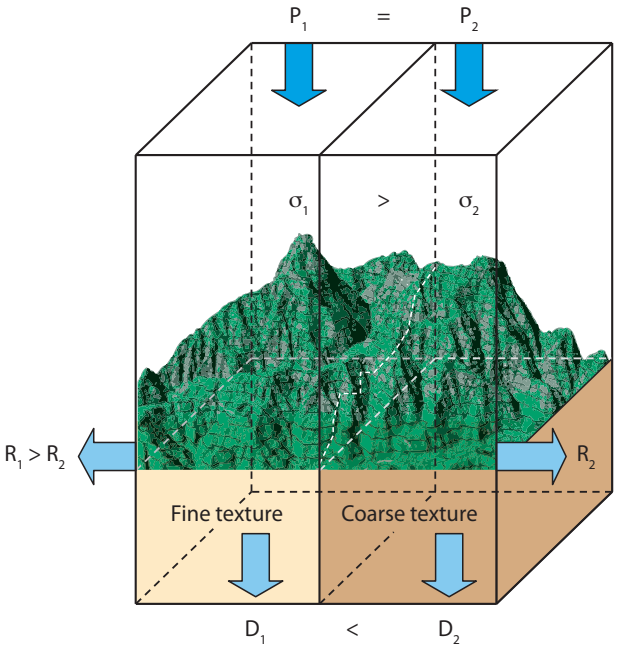

New Leaf Area Index (November 2010)

Boussetta et al. (2011)
- New satellite-based Leaf Area Index

Soil Evaporation (November 2010)

Based on *Mahfouf & Noilhan* (1991)

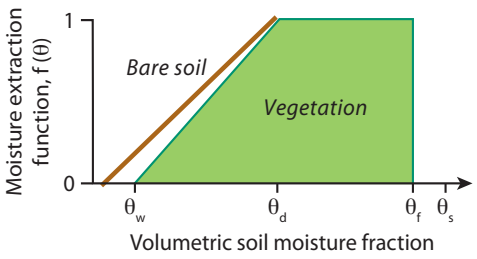

Figure 1 Recent revisions to the land-surface model with the timeline for activation in the operational IFS.

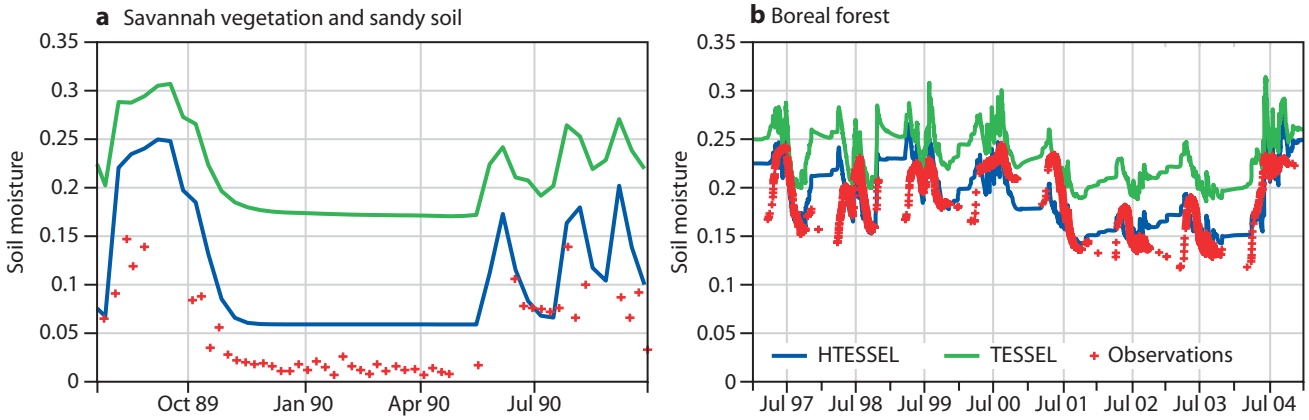

Figure 2 Evolution of soil moisture in TESSEL and HTESSEL in terms of volumetric content (m^3/m^3) compared to observations for two contrasting sites used for field experiments: (a) savannah vegetation and sandy soil (SEBEX, Sahel) and (b) boreal forest (BERMS, Canada).

Vegetation seasonality

The Leaf Area Index (LAI), which expresses the phenological phase of vegetation (growing, mature, senescent, dormant), was kept constant and assigned by a look-up table depending on the vegetation type, thus vegetation appeared to be fully developed throughout the year. To allow for seasonality, a LAI monthly climatology based on a MODIS satellite product has been implemented in IFS Cy36r4 in November 2010. The detailed description of the LAI monthly climatology and its evaluation is provided in *Boussetta et al.* (2011).

Site validation and global offline simulations

The HTESSEL scheme has been compared to TESSEL for the soil moisture evolution on two contrasting field sites (SEBEX Sahel and BERMS Canada, Figure 2), while the HTESSEL+SNOW has been evaluated on forest and open sites (SNOWMIP2 Fraser, US, Figure 3). These results show that the soil moisture simulated by the new model had an improved match to observed values while preserving the soil moisture-evaporation link. Also the snow accumulated on the ground is largely improved by HTESSEL+SNOW scheme, with the snow density playing an important role, both on forest and open-field sites.

The revised land-surface hydrology for both soil and snow has been extensively validated using global offline simulations based on the atmospheric forcing provided by the Global Soil Wetness Project II (GSWP2) covering a 10-year period (1986–1995). A summary of the runoff improvements obtained in the upgrades from TESSEL to HTESSEL and HTESSEL+SNOW for large river catchments in the northern hemisphere is reported in Table 1.

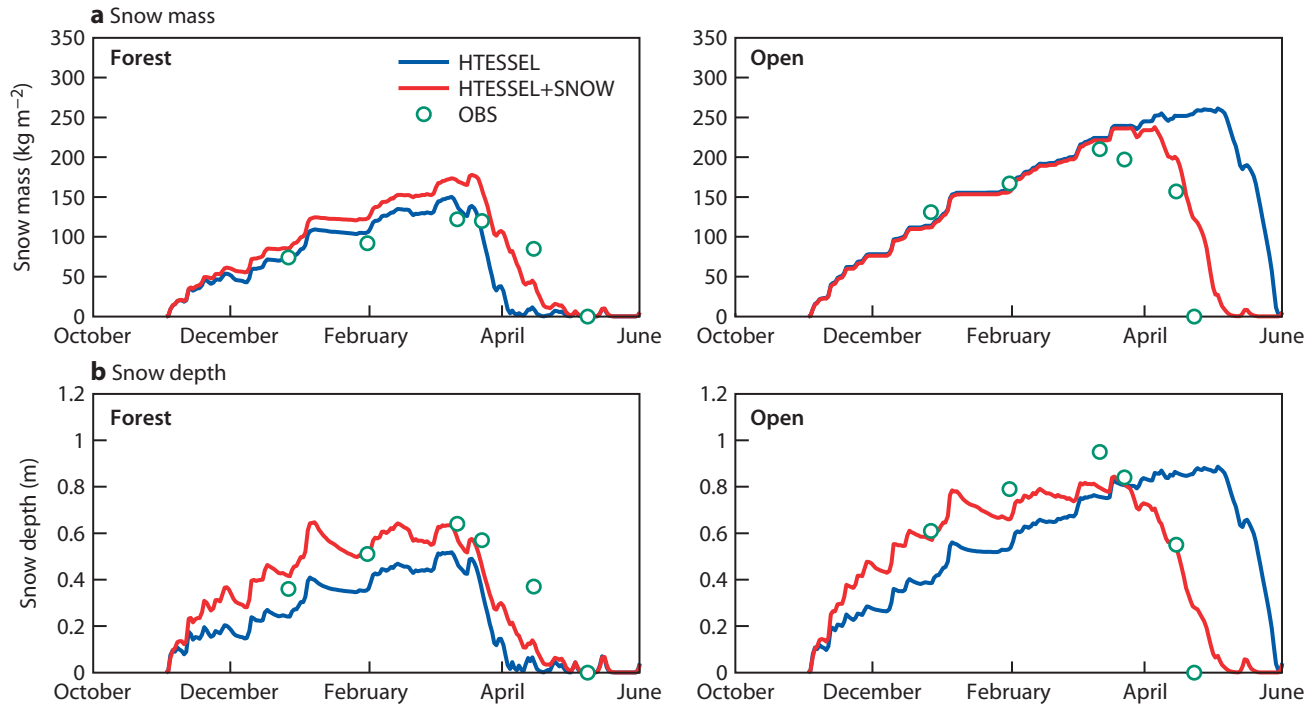

Figure 3 (a) Model-simulated snow mass (in terms of snow water equivalent) and (b) snow depth with HTESSEL and HTESSEL+SNOW during the 2003–04 winter season compared to observations from Fraser forest (left panels) and open (right panels) sites in Colorado that are part of the SnowMIP2 (Snow Model Intercomparison Project).

The runoff error, calculated against observed river-discharges from the Global Runoff Data Centre (GRDC) of the current scheme (including snow and soil revisions), is estimated as 23% of the observed runoff in dominant snow-free basins (over Europe) and 26% in snow-dominated basins. Those results are likely to be affected by the coarse spatial resolution of the simulations (with GSWP2 at a resolution of 1°×1° degrees), but overall they already indicate a substantial increase in predictive skill for monthly river discharges (~33% relative improvement on root-mean-squared-error for the ensemble of river catchments in Table 1).

Forecasts sensitivity experiments

Sets of 10-day forecasts covering one full year have been performed at T399 (~ 50 km horizontal resolution) with the operational IFS (Cy36r1) and TESSEL, HTESSEL, HTESSEL+SNOW and HTESSEL+SNOW+LAI configurations. Forecasts are run 10 days apart to cover the period between the 1 January

Parametrization scheme	Runoff RMSE (mm/day)	Observed area-weighted average runoff from GRDC (mm/day)
Area-weighted average of snow-free basins (~1,632,601 km^2): Northeast-Europe and Central-Europe		
TESSEL	0.28	0.76
HTESSEL	0.17	
Area-weighted average of snow basins (~12,334,161 km^2): Yukon, Podka., Lena, Tom, Ob, Yenisei, Mackenzie, Volga, Irtish and Neva		
HTESSEL	0.75	1.96
HTESSEL+SNOW	0.51	

Table 1 Runoff root-mean-square error (RMSE) for GSWP2 from global offline simulations (1986–1995) verified with GRDC observations on snow-free basins for TESSEL, HTESSEL, and snow-dominated basins for HTESSEL, HTESSEL+SNOW.

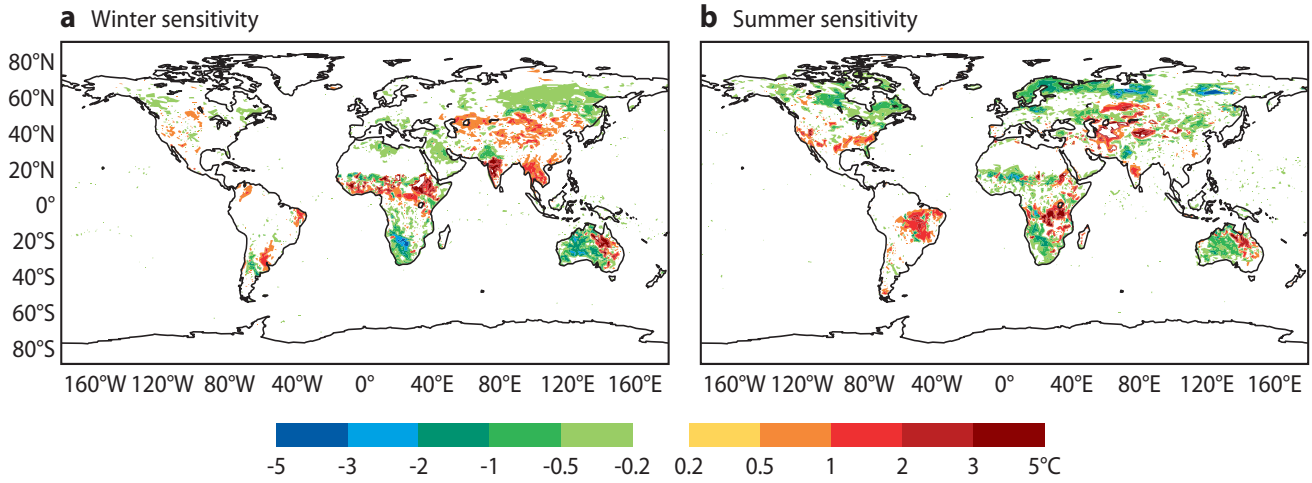

Figure 4 Sensitivity (mean difference) of 36-hour (12 UTC) forecasts of 2-metre temperature for the northern hemisphere (a) winter (December–February) and (b) summer (June–August) for HTESSEL+SNOW compared to TESSEL. Negative values indicate cooling.

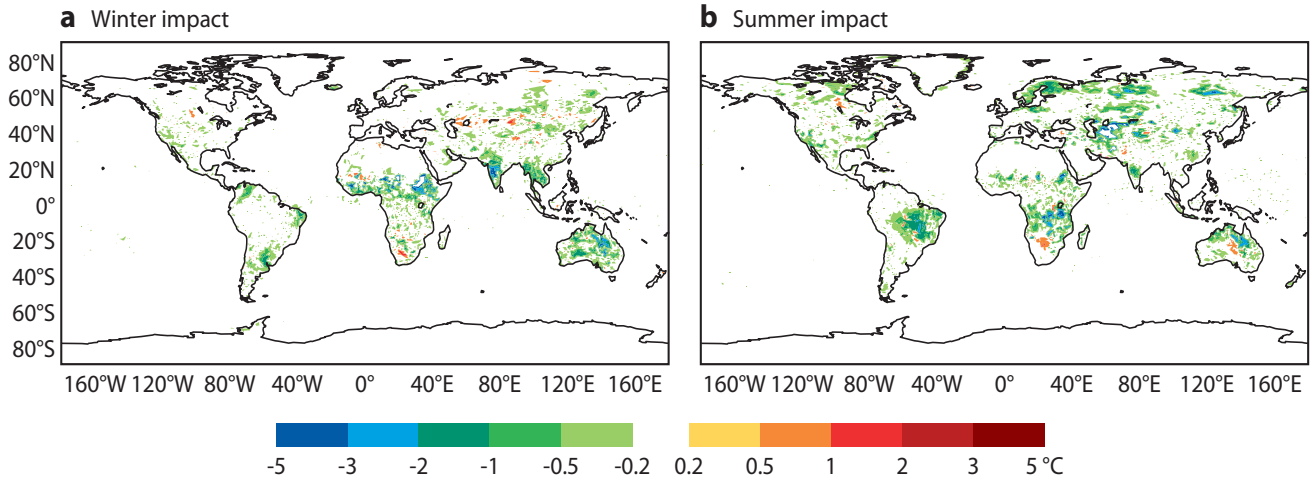

Figure 5 Impact (difference of mean absolute errors) of 36-hour forecasts of 2-metre temperature for the northern hemisphere (a) winter (December–February) and (b) summer (June–August) for HTESSEL+SNOW compared to TESSEL, verified against the ECMWF operational 2-metre temperature analysis. Negative values indicate improvement.

to 31 December 2008 (37 forecasts per experiment). The effect of the model on near-surface temperature is evaluated for short-term (36-hour) forecasts.

The 2-metre temperature 'sensitivity', defined as the mean difference of HTESSEL+SNOW compared to the TESSEL configuration, is shown in Figure 4 for both the winter and summer seasons. The corresponding improvements on 2-metre temperature forecasts 'impact' are shown in Figure 5. The 'impact' is defined as the mean absolute error difference calculated with respect to the operational 2-metre temperature analysis.

HTESSEL particularly improves the temperate climates where evapotranspiration processes are most active. The temperature sensitivity shows positive and negative patterns which are associated to the spatially varying soil texture and the revised soil hydrology.

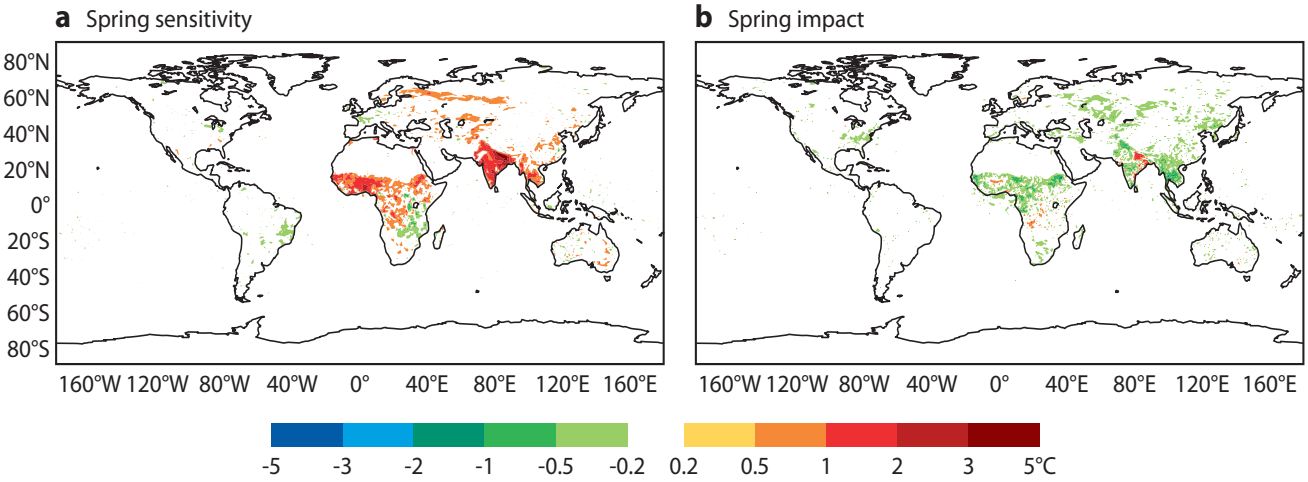

Figure 6 (a) Sensitivity and (b) impact of monthly LAI climatology on 36-hour forecasts of 2-metre termperatures in spring (March–May) as defined in Figures 4 and 5.

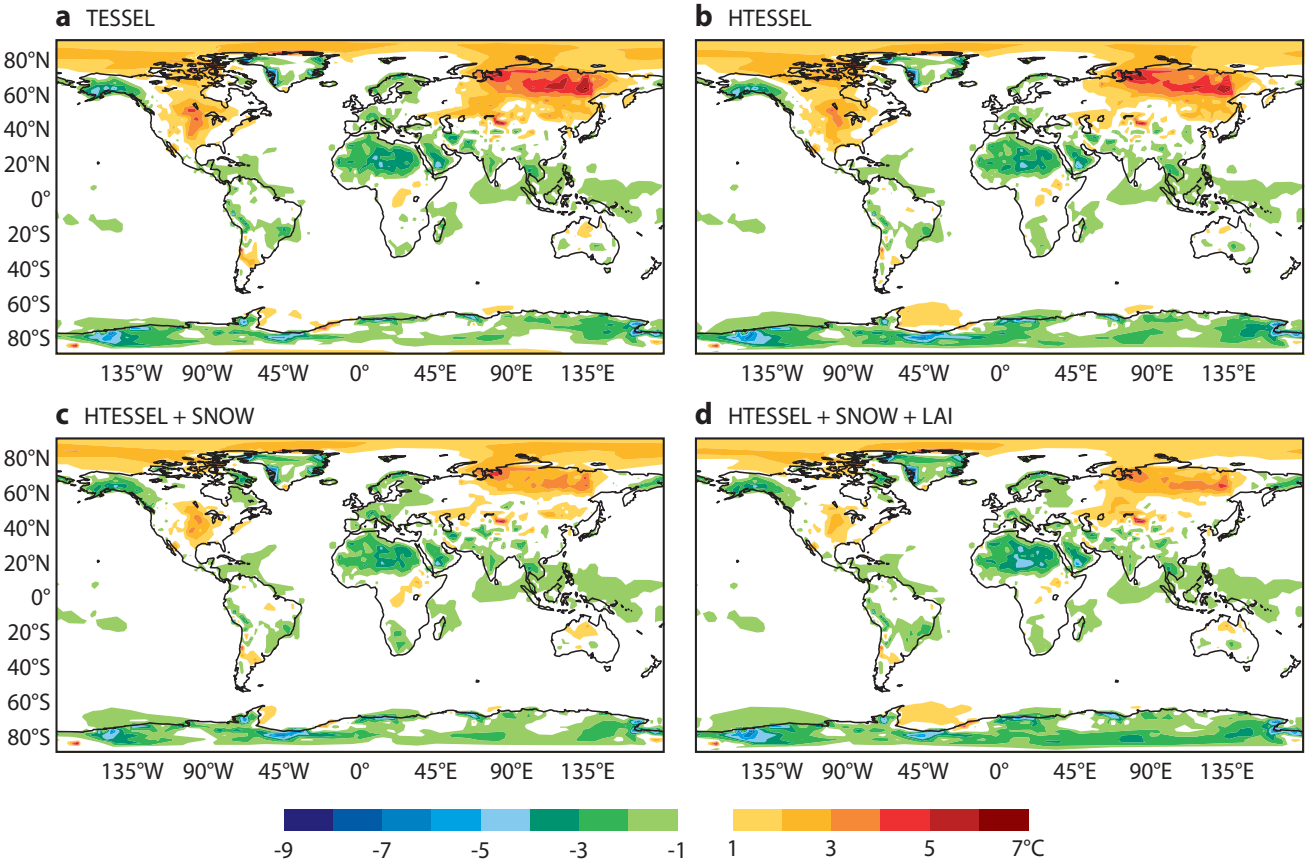

Figure 7 Mean annual 2-metre temperature errors in a long integration compared to ERA-Interim for (a) TESSEL (b) HTESSEL (c) HTESSEL+SNOW and (d) HTESSEL+SNOW+LAI..

The changes introduced in HTESSEL+SNOW are very effective at high latitude and therefore the two revisions have complementary impact (as already demonstrated for the runoff). In fact, the sensitivity at northern latitudes consists of a cooling (Figure 4) associated with the snow pack providing a greater insulation of the soil underneath, and therefore a weaker coupling of the surface to the atmosphere; this has a beneficial impact on near-surface temperature forecasts over snow-dominated regions (Figure 5). The thermal shielding effect of the revised snow has hydrological consequences as the soil remains largely unfrozen and permeable to infiltration also during the cold season. HTESSEL and HTESSEL+SNOW, when coupled to a river routing model (*Pappenberger et al.*, 2009), bring an improved correlation to daily river discharge time-series (*Balsamo et al.*, 2010).

Evaluation of the monthly LAI climatology (HTESSEL+SNOW+LAI) is shown to affect particularly the tropical areas where the seasonality is rather marked due to the monsoon precipitation. The sensitivity indicates generally a warming as shown in Figure 6a for spring as a consequence of lower LAI and reduced evaporation (which provides more energy to the sensible heat flux). At the same time the impact is a reduction of the systematic 2-metre temperature errors, particularly in tropical regions as shown in Figure 6b.

Long integration experiments

Long integration experiments covering one full year with daily specified sea-surface temperatures (hindcasts) are performed at the resolution currently used by the seasonal forecasting system (T159, i.e. ~125 km horizontal resolution). The aim is to assess whether the forecast sensitivities obtained in short-term and medium-range forecasts are also reflected in the climate of the model.

Figure 7 shows the mean annual 2-metre temperature errors with the different land-surface model versions. The 2-metre temperature errors are shown to decrease mostly in areas where the land-surface changes are active and with overall good impact on the model climate.

Outlook

The land-surface model has been revised in its land-surface hydrological components (soil and snow) and in the description of vegetation seasonality (monthly LAI) with positive impact on the forecasts. Future improvements of the land-surface physics will focus on evaporation from free-water surfaces (lakes and intercepted water on leaves). Finally a vegetation/carbon model will be introduced (within the Geoland2 project) to model the net ecosystem exchange of carbon dioxide at the surface.

FURTHER READING

Balsamo, **G.**, **P. Viterbo**, **A. Beljaars**, **B. van den Hurk**, **M. Hirschi**, **A.K. Betts** & **K. Scipal**, 2009: A revised hydrology for the ECMWF model: Verification from field site to terrestrial water storage and impact in the Integrated Forecast System. *Journal Hydrometeorology,* **10**, 623–643.

Balsamo, **G.**, **F. Pappenberger**, **E. Dutra**, **P. Viterbo** & **B. van den Hurk**, 2010: A revised land hydrology in the ECMWF model: A step towards daily water flux prediction in a fully-closed water cycle. Special issue on large scale hydrology of *Hydrol. Process*., doi:10.1002/hyp.7808.

Boussetta, **S.**, **G. Balsamo**, **A. Beljaars** & **J. Jarlan**, 2011: Impact of a satellite-derived Leaf Area Index monthly climatology in a global Numerical Weather Prediction model. *ECMWF Tech. Memo. No. 640*
(submitted to *Int. Journal of Remote Sensing*)

Douville, **H.**, **J.F. Royer** & **J.-F. Mahfouf**, 1995: A new snow parameterization for the Météo-France Climate Model .1. Validation in stand-alone experiments. *Climate Dyn.,* **12**, 21–35.

Dutra, **E.**, **G. Balsamo**, **P. Viterbo**, **P. Miranda**, **A. Beljaars**, **C. Schär** & **K. Elder**, 2010: An improved snow scheme for the ECMWF land surface model: description and offline validation. *J. Hydrometeor.,* **11**, 899–916 (available as *ECMWF Tech. Memo. No. 607*).

Mahfouf, **J.-F.** & **J. Noilhan**, 1991: Comparative study of various formulations of evaporation from bare soil using in situ data. *J. Appl. Meteorol*., **30**, 351–362.

Pappenberger, **F.**, **H. Cloke**, **G. Balsamo**, **T. Ngo-Duc** & **T. Oki**, 2009: Global runoff routing with the hydrological component of the ECMWF NWP system, *Int. J. Climatol.*, doi:10.1002/joc.2028

van den Hurk, **B.**, **P. Viterbo**, **A. Beljaars** & **A.K. Betts**, 2000: Offline validation of the ERA-40 surface scheme. *ECMWF Tech. Memo. No. 295*.

van den Hurk, **B.** & **P. Viterbo**, 2003: The Torne-Kalix PILPS 2(e) experiment as a test bed for modifications to the ECMWF land surface scheme. *Global Planet. Change*, **38**, 165–173.

Viterbo, **P.** & **A. Beljaars**, 1995: An improved land surface parameterization scheme in the ECMWF model and its validation. *J. Climate*, **8**, 2716–2748.

Viterbo, **P.**, **A. Beljaars**, **J.F. Mahfouf** & **J. Teixeira**, 1999: The representation of soil moisture freezing and its impact on the stable boundary layer. *Q. J. R. Meteorol. Soc*., **125**, 2401–2426.

Weisheimer, **A.**, **F. Doblas-Reyes**, **T. Jung** & **T. Palmer**, 2011, On the predictability of the extreme summer 2003 over Europe, *Geophys. Res. Lett.*, **38**, L05704, doi:10.1029/2010GL046455.

Use of SMOS data at ECMWF

JOAQUÍN MUÑOZ SABATER,
PATRICIA DE ROSNAY, ANNE FOUILLOUX

ON 2 November 2009, the Soil Moisture and Ocean Salinity (SMOS) mission was successfully launched from Plesetsk (Russia). This was the second Earth Explorer mission of the European Space Agency (ESA) Living Planet Programme. The most important challenge of this mission is to deliver scientific data with information about the water content of continental surfaces and the salinity content of the oceans. The mission's requirements are to retrieve volumetric soil moisture from the observed radiances with an accuracy of 4% and a spatial resolution of 40–50 km, and salinity in open waters with 0.1 psu accuracy for a 10–30 day average and an open ocean area of 200 km×200 km.

SMOS is a sun-synchronous dawn/dusk polar orbiting satellite flying at an altitude of 758 km. Onboard, a 2D-interferometric radiometer images the entire surface of the Earth between 1.400–1.427 GHz (L-band) once every three days (*Kerr et al.*, 2010). This is the first time that such technology has been used to obtain information about the emission from the surface of the Earth.

SMOS observations can potentially be of great benefit for ECMWF. They are the satellite data most sensitive to soil moisture both with relatively good spatial and temporal resolutions. Although the information they provide is limited to the most superficial soil layer, this data can be assimilated in the Extended Kalman Filter (EKF) soil moisture analysis of ECMWF (*Drusch et al.*, 2008, *de Rosnay et al.*, 2011) to correct the value of the root-zone soil moisture. A better initialization of the root-zone soil moisture has proven to have an impact on short- to medium-range weather forecasts (*Ferranti & Viterbo*, 2006). Currently, the EKF is used operationally at ECMWF to adjust the soil moisture state through the assimilation of 2-metre temperature and relative humidity observations.

The SMOS team working at ECMWF provides operational monitoring of SMOS data and the next objective is to assimilate this data using the EKF. For SMOS, continuous monitoring in near real time (NRT) is especially important. This is because the ambitious technique used to extract information about soil moisture and ocean salinity needs to be tested and validated before an operational mission can be designed. For ECMWF, the main objective will be to investigate the ability of SMOS data to improve the forecast skill.

Why a passive mission in L-band to sense soil moisture?

Over the last two decades, remotely-sensed microwave observations from 1 to 10 GHz have been used to obtain information about the water content of a shallow near-surface layer. In this microwave region, attenuation from clouds and vegetation is smaller than at higher frequencies. Remote sensing of soil moisture (as with many other variables) can be carried out for two types of sensors: active and passive. Active instruments emit an electromagnetic pulse to illuminate the scene they observe. Then they measure the radiation that is reflected or backscattered from that scene. In contrast, passive instruments measure directly the radiation emitted by the Earth. Factors such as vegetation or soil roughness are less significant in passive remote sensing of microwaves. In addition, L-band has the advantage of having little sensitivity to the water vapour in clouds and rain in the atmosphere, even for adverse weather conditions. Therefore SMOS (using a passive L-band instrument) should have the capability to monitor the soil moisture under conditions where other sensors have problems.

The high cost and technological challenge of arranging a large antenna in L-band has prevented an earlier mission based on this technology. For SMOS, an antenna of approximately 8 metres in diameter is necessary to comply with the spatial resolution requirements of the mission. In SMOS this problem has been overcome by applying the interferometric technique. Instead of one large antenna, sixty nine small receivers installed in three arms collect the radiation emitted by the Earth's surface between 1.400 and 1.427 GHz. By combining the signals received by the small receivers, a two-dimensional image of the Earth's surface brightness temperature (which is proportional to the radiation emitted by the surface) can be reconstructed.

ECMWF will use SMOS data in synergy with active measurements, in particular with a global soil moisture index product derived from the C-band (5.255 GHz) active microwave data of the Advanced Scatterometer instrument (ASCAT), onboard the MetOp platform, to better constrain the soil moisture state.

Which product is used at ECMWF?

ECMWF is receiving the data from the SMOS Data Processing Ground Segment in NRT. It constitutes geographically sorted swath-based maps of brightness temperatures. The geolocated product received at ECMWF is arranged in an equal-area grid system called ISEA 4H9. For this grid, the centres of the cell grids have almost an equal spacing of 15 km over land. Over oceans the grid has a coarser resolution, which is half of the resolution over land, as oceans are more homogeneous than continental surfaces.

The data arrives organized in snapshots, each being generated every 1.2 seconds. After the end of the commissioning phase it was decided that SMOS would measure in the so called full polarization mode. This means that for the first 1.2 seconds all the receivers in the three arms are in the same polarisation mode (and then obtaining pure horizontal or vertical polarized observations; i.e. when the

orientation of the electric field of the electromagnetic waves received at the three arms is parallel or perpendicular to the satellite antenna reference frame, respectively), whereas in the following 1.2 seconds the receivers in an arm switch the polarisation. For the first 1.2 seconds approximately 4,800 observations are found within a snapshot, whereas this quantity can be doubled in the next 1.2 seconds. Each of these observations is provided in a node (or grid point) of the ISEA grid.

Developments towards an operational monitoring chain

To take full advantage of the NRT product, ECMWF implemented this new data type within the Integrated Forecasting System (IFS). This was a challenging task for several reasons. For SMOS, the interferometric technique observes the same area at different angles as the satellite moves along the track. Up to 150 records of brightness temperatures observed at incidence angles between 0° and 65° are provided for each location. So the angular resolution of the observations is very high. This measuring principle has two consequences: (a) it provides a unique dataset with new features very different to any other source of satellite data used for NWP and (b) it produces a very large volume of data which cannot all be ingested into the IFS. This raises a great concern about the feasibility of integrating SMOS data in the IFS. However, SMOS data is still compatible with the current structure of the IFS if the amount of data is significantly reduced. Data thinning is essential in this context. The thinning approach for SMOS data needs to avoid redundant observations and reduce drastically the volume of the original dataset, while keeping the angular distribution of the observations.

From the more than 8 Gb of daily data that can reach ECMWF archives, only 5 to 10% can realistically be ingested into the IFS. An optimal trade-off between number of incidence angles and volume of data is to keep only six incidence angles with a margin of ±0.5°. These angles are 10°, 20°, 30°, 40°, 50° and 60°. They are continuously being monitored and the results are publicly available in NRT at:

- http://www.ecmwf.int/research/ESA_projects/SMOS/monitoring/smos_monitor.html.

This is an excellent tool to assess and analyse the angular and polarised evolution of the data as a function of time. For more detailed information see *Sabater et al.* (2009, 2010).

The forecast model's estimate of the SMOS data (the model equivalent) is computed at the model grid points. In the case of SMOS, this has several advantages.

- All the background fields necessary to simulate brightness temperatures at the top of the atmosphere are computed and available at model grid points. Thus, it avoids interpolating physical quantities to observation location.
- Other satellite data sensitive to soil moisture, such as AMSR-E data in C-band, is also available at model grid points, making a comparison possible with other satellite data.

The Community Microwave Emission Model (CMEM) is currently used to simulate the soil emission in L-band. Further information about CMEM and its current configuration can be found at:

- http://www.ecmwf.int/research/ESA_projects/SMOS/cmem/cmem_index.html.

Monitoring results

Daily monitoring of observed brightness temperatures

SMOS data has been regularly monitored since the launch of the satellite. Daily maps of brightness temperatures have been produced and published on the ECMWF SMOS website mentioned above. These maps were especially of interest during the commissioning phase when a series of calibration events took place. As an example, Figure 1a shows global maps of brightness temperatures at 40° incidence angle for the vertical polarisation, as measured by SMOS, on 28 November 2009. This data corresponded to data from the 'Switch-On Phase'. Figure 1b shows data approximately four weeks later, on 20 December 2009, just after a major calibration event took place.

The plots in Figure 1 clearly show a significant improvement in the quality of the observations. The early mission data was very noisy (presented as dark red in the Figure 1a) and with significant geo-location problems, which was completely normal at that phase. However, the data in late December (Figure 1b) was of much better quality and more in agreement with expectations. Furthermore, the edges of the satellite track looked colder than the inner part. This is the area which corresponds to the extended alias-free field of view (EAFOV), which is a post-processed area to benefit from global coverage every three days, but with the drawback of being of lesser quality. These plots were useful to observe anomalies in the data, especially important during the commissioning phase. They were supported until November 2010. From this date onwards, global statistics have been produced in NRT.

Difference between observations and model equivalents

It is important to monitor the difference between observations and model equivalents (also called first-guess departures). They typically follow a normal distribution with mean value relatively close to zero. This result is very positive as it means that in average ECMWF L-band simulated brightness temperatures are in good agreement with SMOS data. However, the probability distribution functions of first-guess departures also have long tails at both sides, suggesting that a significant number of large differences between model equivalents and observations are still present. The largest wet biases are found in areas with strong orography. This result was expected as the capabilities of CMEM for areas with strong slope, snow and ice are currently inaccurate. The emission over boreal forests, ice and snow covered areas is also significantly overestimated by CMEM. In particular, the snow line over continental surfaces can be monitored very well using the mean values of first-guess departures, as shown in Figure 2.

Concerning the large dry bias, there seems to be two main regions affected: (a) the area near coastlines, where the observed brightness temperatures are strongly

influenced by sea water (with much lower values of brightness temperature), and (b) over dry areas observed at large incidence angles. It is well known that roughness effects are not yet well modelled for large incidence angles at the L-band, and in particular for the more sensitive horizontal polarisation. Recent analyses have shown a significant reduction of the tails in the histograms of first-guess departures. The reason is twofold: on the one hand, recent calibrations of the instrument have improved the quality of the observations; on the other hand, the improved model physics used in the current cycle has also improved the ECMWF model equivalents. In particular, the introduction into the IFS cycle 36r4 of a new improved bare soil evaporation scheme, producing more realistic dry values of the soil water content over bare soil, has a significant impact on the ECMWF model equivalents.

Data over oceans

SMOS data is not only being continuously monitored for land masses, but also for oceans. The current L-band emission model over oceans used at ECMWF is quite simple and does not account for contributions due to the galactic noise (which is an ever-present background cosmic radiation, see the figure in Box A) or roughness caused by ocean winds. However, observed radiances have shown a very good correlation with areas covered in sea ice.

Figure 3 shows the average brightness temperatures in grid-boxes of 1° from 5 to 19 November 2010. It can be observed that on average the polar latitudes have higher brightness temperatures than the rest of the oceans. This is the combination of several factors: firstly the water in these zones is colder and fresher with lower salinity (factors which have an influence over the water emission in L-band), but the main reason is due to the sea ice near the poles. Over ice-covered areas the surface emits as if it was drier, which results in substantially higher brightness temperatures. The average brightness temperatures over oceans are very well correlated with maps of sea ice cover; this confirms the ability of SMOS data to also monitor sea ice.

Main problems of the SMOS data

The innovative instrument onboard of SMOS has had to face various problems. The galactic radiation, to which the satellite is continuously being subjected, was the origin of several problems related to the memory (which temporally stores the data in the satellite) and the frequency imbalances of the instrument. More recently, an increase of the temperature of one of the main antennas was observed, thus producing an unwanted trend in the temporal evolution of the brightness temperatures. This is currently under investigation. However, all these problems can be considered small compared to the Radio Frequency Interference (RFI). SMOS data is significantly contaminated by anthropogenic sources in the protected L-band. Many of these sources have a civilian origin, such as radio links, wi-fi networks or surveillance cameras. Efforts made by various ESA teams have made it possible to switch off around 50 sources in Europe which were strongly contaminating the observations.

a 28 November 2009

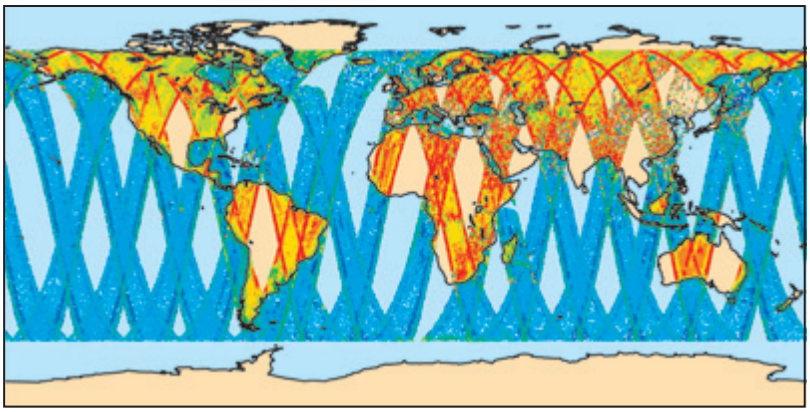

b 20 December 2009

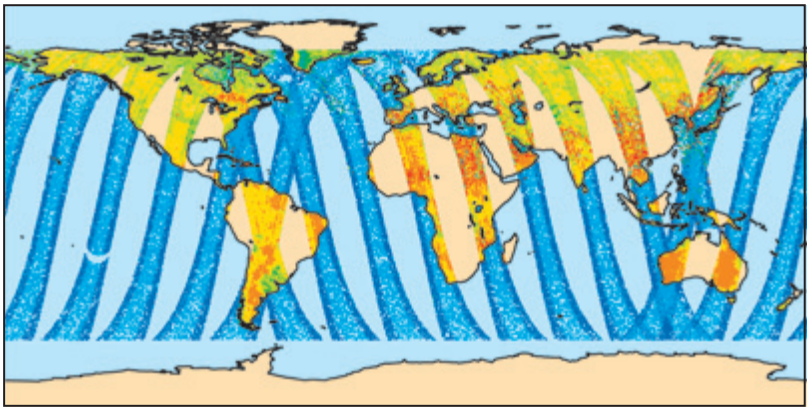

Figure 1 Observed SMOS brightness temperatures (K) at 40° incidence angle and vertical polarisation on (a) 28 November 2009 and (b) 20 December 2009.

How can soil moisture be retrieved from SMOS observations?

A

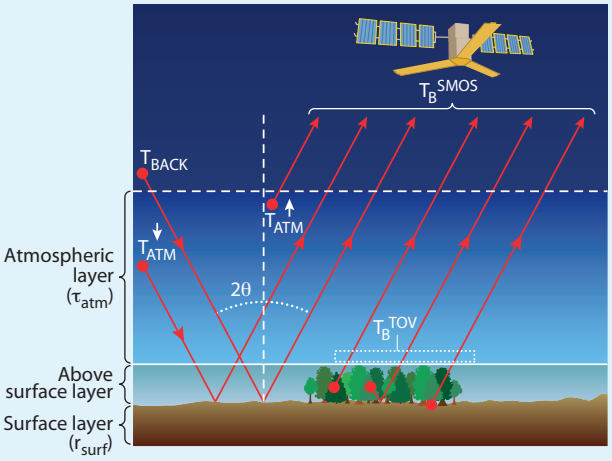

The SMOS observation system is a microwave imaging radiometer with aperture synthesis. It collects top-of-the-atmosphere radiances coming from the scene viewed by the SMOS antennas. At the frequency operated by SMOS (1.4 GHz), the brightness temperature (defined as the temperature a blackbody would be in order to produce the radiance received by the sensor) and radiances are directly proportional. Thus, as it is done for many other satellite data, SMOS data is expressed in terms of brightness temperatures rather than in radiances as the units of temperature are easier to interpret than the units of radiances.

The brightness temperatures sensed by the SMOS antennae (T_B^{SMOS}) results from several contributions: (a) surface emission (T_B^{TOV}) attenuated by the atmosphere (τ_{ATM}), (b) the up-welling atmospheric emission ($T_{ATM}^{\uparrow}$), (c) the down-welling atmospheric emission ($T_{ATM}^{\downarrow}$) reflected at the surface and attenuated by the atmosphere, and (d) the cosmic background emission (T_{BACK}) attenuated by the atmosphere, reflected at the surface (r_{SURF}) and attenuated again by the atmosphere. Among all of these contributions, T_B^{TOV} is the most important one. It takes into account the soil emission as well as the emission and the attenuation effects of the vegetation. Soil roughness or the presence of snow also affect the surface emissivity.

The emissivity of the surface is the key variable to retrieve soil moisture. The surface emissivity can be expressed as a function of the dielectric constant of the surface. However, the surface dielectric constant is very different between a dry soil and a wet soil. Detection of soil moisture from a remote sensing platform is based on this principle. The sensitivity of the soil emissivity to soil moisture is optimal at L-band and, although with different magnitude, this is valid for both the horizontal and the vertical polarization. By combining the data from both polarizations unwanted effects in the signal can be removed and soil moisture can be retrieved more accurately.

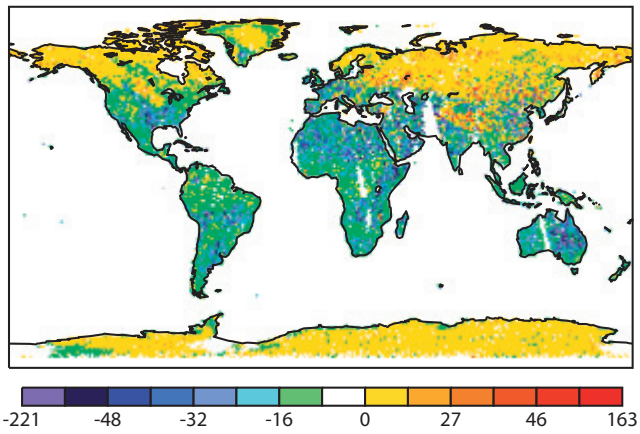

Figure 2 Averaged first-guess departures of brightness temperatures (K) for the first week of March 2010 at 1° spatial resolution. Only observations with an incidence angle of 50° and horizontal polarization are considered in this figure.

In Figure 4, the variability of the observations averaged over a week is shown. This figure presents complex patterns related to the state of the soil variables. However, there are some areas mainly in the East of Europe and Asia that present abnormally large variability (in red in the figure). This cannot be explained by the geophysical variability of the observations, but rather by external sources related to RFI.

RFI is not only limited to continental surfaces. Figure 5 shows the average variability of the observations between 5 and 19 November 2010 over oceans. A significant land-sea contamination is observed. There is a very large contamination around the European and Asiatic coasts caused by strong RFI sources over land, which can contaminate the observations up to several hundreds of kilometres offshore. This effect is sharper with increasing incidence angle. To a lesser extent, SMOS observations over sea are also affected in a well-defined latitudinal band of North America due to a series of military radars. Other point sources of RFI are also distributed in several locations over the ocean. The interface between sea ice and open sea water, showing extraordinary dynamics, is also very well captured in this figure, as it can be clearly seen near the south pole. The reason for this is the strong contrast in brightness temperatures between open sea water and water covered by sea ice.

Although the best approach to avoid RFI contamination is to directly switch off the illegal sources at the L-band, this is a slow process as it means requesting the national management authorities to ensure that citizens comply with the International Telecommunication Union regulations. In some countries this is a very difficult process. Currently, several detection and mitigation algorithms are being developed to reduce the impact of RFI on the observations.

Way forward

The potential benefit that the assimilation of SMOS data could bring to the forecast skill will strongly depend on the thinning approach applied to the observations. It is important to try to understand which subset of data carries most information about the soil water content. In addition, SMOS

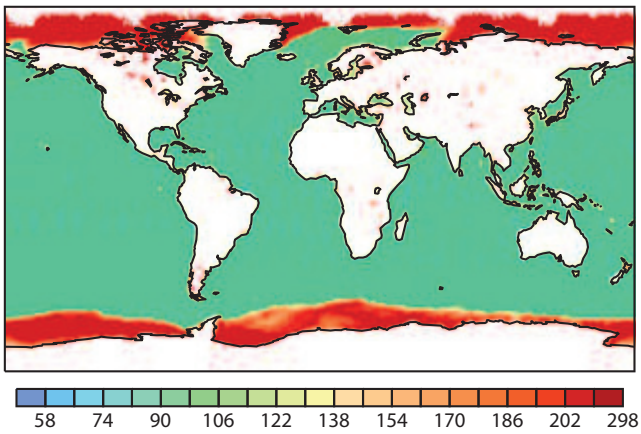

Figure 3 Average SMOS brightness temperatures (K) over oceans at 1° spatial resolution from 5 to 19 November 2010 at a 40° incidence angle and for the vertical polarisation.

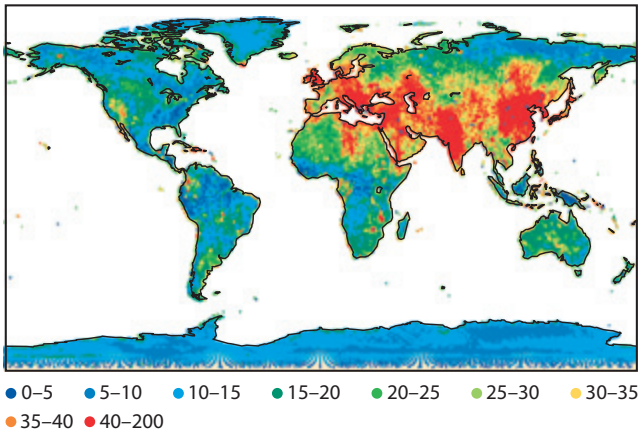

Figure 4 Average standard deviation of the SMOS observed brightness temperatures (K) the first week of October 2010 at horizontal polarization and 40° incidence angle.

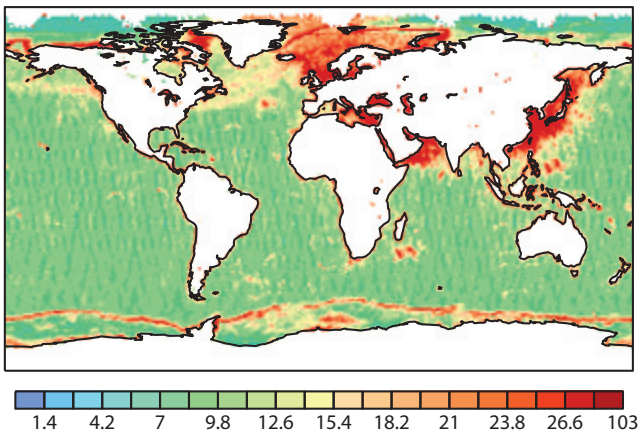

Figure 5 Average of the standard deviation of the SMOS observed brightness temperatures (K) over oceans at 40° incidence angle for the vertical polarisation mode for the period 5 to 19 November 2010.

observations are quite noisy as the size of the observed (very heterogeneous) surface of the Earth is very different depending on the incidence angle.

Not only is the optimal use of SMOS data being investigated in view of its assimilation, but also the reduction of noise and significant spatial correlations observed between adjacent observations are being studied. A bias correction scheme, likely based on physical parameters such as roughness or vegetation, will also be developed. It is also envisaged to reduce the bias between SMOS observations and the model equivalent by performing a global calibration of the CMEM parameters which have the strongest influence on the simulated brightness temperatures. The current configuration of the CMEM is based on research which investigated different aspects of the soil emission at local or regional scales. A global re-processed SMOS dataset performed by ESA will be used for validation purposes.

Finally, all these activities, which are aimed at optimally preparing the data for assimilation in the EKF, will be the base for testing the impact that the assimilation of SMOS data has on the forecast skill. This will be tested under several assimilation configurations combining screen-level variables and SMOS data.

FURTHER READING

de Rosnay, P., M. Drusch, G. Balsamo, C. Albergel & **L. Isaksen**, 2011: Extended Kalman Filter soil-moisture analysis in the IFS. *ECMWF Newsletter No. 127*, 12–16.

Drusch, M., K. Scipal, P. de Rosnay, G. Balsamo, E. Andersson, P. Bougeault & **P. Viterbo**, 2008: Exploitation of satellite data in the surface analysis. *ECMWF Tech. Memo. No. 576*. http://www.ecmwf.int/publications/library/do/references/show?id=88712

Ferranti, L. & **P. Viterbo**, 2006: The European summer of 2003: Sensitivity to soil water initial conditions. *J. Climate*, **19**, 3659–3680.

Kerr, Y., P. Waldteufel, J.-P. Wigneron, S. Delwart, F. Cabot, J. Boutin, M.-J. Escorihuela, J. Font, N. Reul, C. Gruhier, S.E. Juglea, M. Drinkwater, A. Hahne, M. Martin-Neira & **S. Mecklenburg**, 2010:The SMOS mission: new tools for monitoring key elements of the global water cycle. In *Proc. IEEE 2010*, 98, 666-687, doi:10.1109/JPROC.2010.2043032.

Sabater, J.M., P.de Rosnay, A.Fouilloux, M. Dragosavac & **A. Hofstadler**, 2009: IFS interface. *M1TNP2 ESA Technical Report*. http://www.ecmwf.int/publications/library/do/references/show?id=89524

Sabater, J.M., P. de Rosnay & **A. Fouilloux**, 2010: Operational Pre-processing chain, Collocation software development and Offline monitoring suite. *M2TNP1/2/3 ESA Technical Reports*. http://www.ecmwf.int/publications/library/do/references/show?id=89972

Support for OGC standards in Metview 4

SÁNDOR KERTÉSZ, STEPHAN SIEMEN, FERNANDO II

THE OPEN Geospatial Consortium (OGC) defines a number of standards for serving and retrieving geospatial data over the web. These standards have become increasingly popular over the last decade since they can offer an easy way for organisations within different domains to share geospatial information and thus enhance interoperability. In the meteorological domain these standards open up new possibilities, such as exchanging observations and forecast data with other user domains and showing meteorological and non-meteorological data together (see Box A).

To support the meteorological community in adopting the OGC standards, the MetOcean Domain Working Group was established within the OGC. ECMWF is an active participant of this working group and this article briefly describes the development within Metview 4 to support OGC standards.

Keyhole Markup Language

The Keyhole Markup Language (KML) format was originally developed for use within Google Earth and later it became an official standard of the OGC. At present, KML is widely used to define two- or three-dimensional geospatial information that can be displayed in Google Earth, Google Maps and other similar applications. Metview 4 offers various ways of supporting KML. First, KML files are represented by an icon in the Metview desktop, which users can *edit* and *visualise* with an external viewer (by default it is Google Earth – see Figure 1). Secondly, through its use of Magics++ for its plotting, geographical contour plots can be written in KML format both in the interactive user interface and in Metview Macro. Lastly, Geopoints files, which are Metview's custom format to store scattered georeferenced data, can be converted into KML using the *GeoToKML* module (Figure 2a).

Web Map Service

OGC's Web Map Service (WMS) standard focuses on the generation and retrieval of geo-referenced map images over the web. A key concept of WMS is that of a layer representing a basic unit of geographical information that a WMS client can request as a map image from a WMS server. A client can send at least two types of requests to the server: a *GetCapabilities* request, to acquire information about the available layers, and a *GetMap* request, to generate a map image for a particular layer using a specified geographic co-ordinate reference system and graphical style. As for the visualisation, this means that the client can be relatively simple since it only has to deal with static map images, while the hard and complex task of data access and map image rendering is performed by the server.

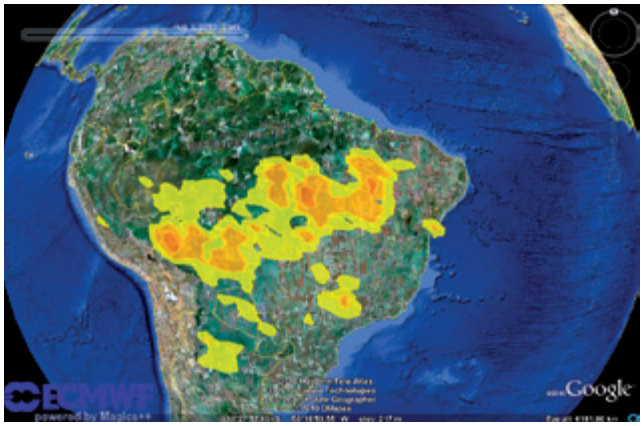

Figure 1 Snapshot of Google Earth showing the biomass burning product of the MACC (Monitoring Atmospheric Composition and Climate) project visualised through KML generated by Metview (download from http://gmes-atmosphere.eu/fire).

Users of WMS should be aware that not all providers guarantee the availability of their services, and network status and bandwidth can also affect performance.

WMS client in Metview 4

Client-Server architectures, such as used in WMS, fit very well into the service-oriented design of Metview. The Metview WMS client, whose icon can be seen in Figure 2b, was designed as a standard Metview module to provide an easy and powerful way to incorporate WMS map images into the Metview environment. The client offers a high-level user interface to build and perform the *GetMap* request. Also it is able to send the resulting map images to Metview's Display Window, which can overlay them with other sources of data.

The WMS icon editor provides two ways for users to generate a GetMap request: an interactive and a plain mode. In the interactive mode the editor resembles a web browser as shown in Figure 3. Once the WMS server's URL is typed in at the top of the interface, the client performs the *GetCapabilities* request and populates the user interface with the resulting list of layers and their meta-data. The available layer hierarchy is shown in the left-hand pane. When a layer is selected its properties can be further specified by the users: the map portrayal style and the various layer dimensions, which can typically specify the time and elevation of the layer, can all be set. Users can

a  b 

Figure 2 Icons representing the GeoToKML module and WMS client in Metview 4.

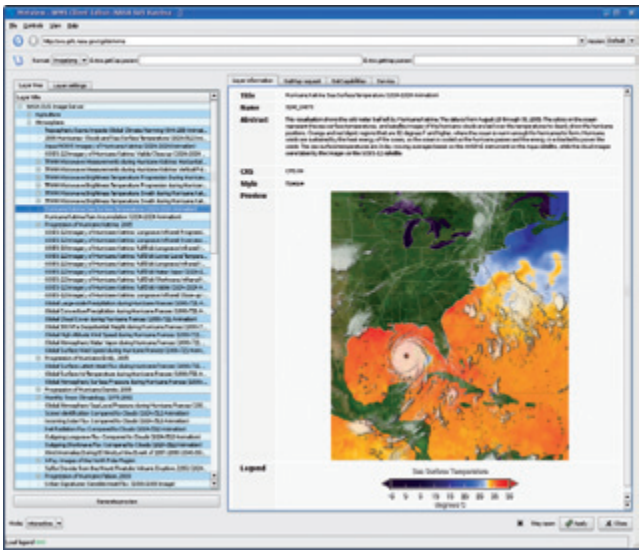

Figure 3 The WMS client's user interface in interactive mode to select and preview the layers provided by a WMS server, in this case NASA's Science Visualization Studio. The layer selected here is a composite image from various satellites showing the cloud system of Hurricane Katrina and the sea surface temperature.

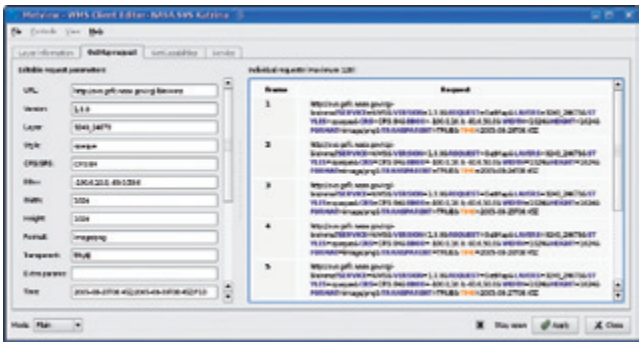

Figure 4 The WMS client's user interface in plain mode allowing the manual editing of the GetMap request.

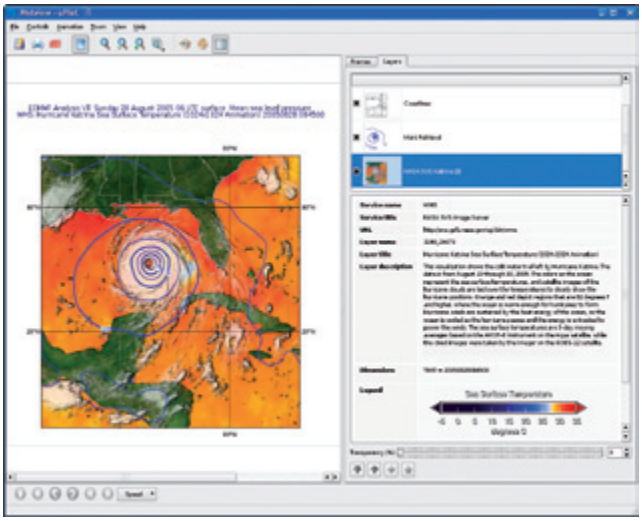

Figure 5 The WMS map image visualised in Metview 4, based on the GetMap request shown in Figure 4, overlaid with the corresponding mean-sea-level pressure analysis from ECMWF's MARS archive.

generate a preview at any time to see how the map image would look if the current settings were used. This preview, complemented with various layer meta-data, is displayed in the right-hand pane.

The *GetMap* request itself, built by the client, can also be inspected in the user interface but users need to switch to the plain editor mode to be able to manually change the request (Figure 4).

Once the *GetMap* request is defined it can be run and visualised by either right-clicking on the icon and selecting *visualise* from the context menu or simply dropping the icon into an existing Metview plot. The resulting WMS map image appears in Metview's Display Window and can now be overlaid with any other Metview charts (Figure 5). The meta-data associated with the WMS map image is displayed in the Layers tab of the display window.

Metview users will find a tutorial that goes into more detail how to use the WMS client on the Metview documentation web page at:

- http://www.ecmwf.int/publications/manuals/metview/documentation.html

The WMS client has been extensively used to test ECMWF's new WMS server (see the article in *ECMWF Newsletter No. 126*, 23–27) and to contribute to the work of the MetOcean Domain Working Group at the OGC. In this context, tests with various servers were made whose outcome is documented at the MetOcean DWG webpage at:

- http://external.opengis.org/twiki_public/MetOceanDWG/MetocWMS_WMS_IE_Retex

Ongoing work

Work on Metview's WMS client is still ongoing with a special focus on the support for various geographical co-ordinate reference systems and the caching of the WMS images. Parallel to this work clients are under development to access remote services of gridded data, similar to the MARS retrieval module. To be compatible with the EU INSPIRE directive, which establishes an infrastructure for spatial information in Europe to support environmental activities, it is also planned to access catalogue services from within Metview.

Meteorology and Oceanography Domain Working Group

A

The Meteorology and Oceanography Domain Working Group (Met Ocean DWG) is a community orientated working group of the Open Geospatial Consortium (OGC). The group does not directly revise OGC standards, but rather enables collaboration and communication between groups with meteorological and oceanographic interests.

The Met Ocean DWG maintains a list of topics of interest to the meteorological and oceanographic communities for discussion, defining feedback to the OGC Standards Working Groups (SWG), and performing interoperability experiments.

ECMWF Calendar 2011

September 6 – 9	Seminar on 'Data assimilation for atmosphere and ocean'
September 26 – 28	Introduction to ECflow for SMS users
October 3 – 5	Scientific Advisory Committee (*40th Session*)
October 5 – 7	Technical Advisory Committee (*43rd Session*)
October 10 – 14	Training Course – Use and interpretation of ECMWF products for WMO Members
October 10 – 11	Finance Committee (*89th Session*)
October 12 – 13	Policy Advisory Committee (*32nd Session*)
October 17	Advisory Committee of Co-operating States (*17th Session*)
October 19	RMetS/EMS meeting on 'Why aerosols matter: Advances in observations, modelling and understanding impacts'
October 31 – November 4	13th Workshop on 'Meteorological operational systems'
November 8 – 10	Workshop on 'Diurnal cycles and the stable atmospheric boundary layer (GABLS)'
December 6 – 7	Council (*76th Session*)

ECMWF publications (see http://www.ecmwf.int/publications/)

Technical Memoranda

646 **Pinson, P. & R. Hagedorn**: Verification of ECMWF ensemble forecasts of wind speed against observations. *March 2011*

645 **Engelen, R. & P. Bauer**: The use of variable CO_2 in the data assimilation of AIRS and IASI radiances. *March 2011*

644 **Masiello, G., M. Matricardi & C. Serio**: The use of IASI data to identify systematic errors in the ECMWF forecasts of temperature in the upper stratosphere. *March 2011*

642 **Lu, Q., W. Bell, P. Bauer, N. Bormann, C. Peubey & A. Geer**: Improved assimilation of data from China's FY-3A Microwave Temperature Sounder (MWTS). *February 2011*

641 **Lu, Q., W. Bell, P. Bauer, N. Bormann & C. Peubey**: Characterising the FY-3A microwave temperature sounder using the ECMWF model. *February 2011*

640 **Boussetta, S., G. Balsamo, A. Beljaars, T. Kral & L. Jarlan**: Impact of a satellite-derived Leaf Area Index monthly climatology in a global Numerical Weather Prediction model. *April 2011*

636 **Isaksen, L., M. Bonavita, R. Buizza, M. Fisher, J. Haseler, M. Leutbecher & L. Raynaud**: Ensemble of data assimilations at ECMWF. *December 2010*

635 **Richardson, D.S., J. Bidlot, L. Ferranti, A. Ghelli, T. Hewson, M. Janousek, F. Prates & F. Vitart**: Verification statistics and evaluations of ECMWF forecasts in 2009–2010. *October 2010*

EUMETSAT/ECMWF Fellowship Programme

22 **Di Tomaso, E. & N. Bormann**: Assimilation of ATOVS radiances at ECMWF: first year EUMETSAT fellowship report. *March 2011*

21 **Lupu, C. & A. McNally**: Assimilation of radiance products from geostationary satellites: 1-year report. *February 2011*

ERA Report Series

11 **Král, T.**: Flux tower observations for the evaluation of land surface schemes: Application to ERA-Interim. *April 2011*

10 **Kållberg, P.**: Forecast drift in ERA-Interim. *April 2011*

8 **Haimberger, L. & U. Andrae**: Radiosonde temperature bias correction in ERA-Interim. *February 2011*

9 **Dee, D.P., S.M. Uppala, A.J. Simmons, P. Berrisford, P. Poli, S. Kobayashi, U. Andrae, M.A. Balmaseda, G. Balsamo, P. Bauer, P. Bechtold, A.C.M. Beljaars, L. van de Berg, J. Bidlot, N. Bormann, C. Delsol, R. Dragani, M. Fuentes, A.J. Geer, L. Haimberger, S. Healy, H. Hersbach, E.V. Hólm, L. Isaksen, P. Kållberg, M. Köhler, M. Matricardi, A.P. McNally, B.M. Monge-Sanz, J.-J. Morcrette, C. Peubey, P. de Rosnay, C. Tavolato, J.-N. Thépaut & F. Vitart**: The ERA-Interim reanalysis: Configuration and performance of the data assimilation system. *February 2011*

ESA Contract Reports

Abdalla, S.: Global validation of ENVISAT wind, wave and water vapour products from RA-2, MWR, ASAR and MERIS (2008-2010). Contract 21519/08/I-OL. *April 2011*

Munoz Sabater, J., P. de Rosnay & M. Dahoui: SMOS continuous monitoring report – Part 1. Contract 20244/07/I-LG. *February 2011*

Dragani, R.: Monitoring and assimilation of SCIAMACHY, GOMOS and MIPAS retrievals at ECMWF. Technical support for global validation of ENVISAT data products. Contract 21519/08/I-OL. *February 2011*

Index of newsletter articles

This is a selection of articles published in the *ECMWF Newsletter* series during the last five years.
Articles are arranged in date order within each subject category.
Articles can be accessed on the ECMWF public website – www.ecmwf.int/publications/newsletter/index.html

Useful names and telephone numbers within ECMWF

Telephone

Telephone number of an individual at the Centre is:

International: +44 118 949 9 + three digit extension
UK: (0118) 949 9 + three digit extension
Internal: 2 + three digit extension

e.g. the Director-General's number:
+44 118 949 9001 (international),
(0118) 949 9001 (UK) and 2001 (internal).

E-mail

The e-mail address of an individual at the Centre is:
firstinitial.lastname@ecmwf.int

e.g. the Director-General's address: D.Marbouty@ecmwf.int

For double-barrelled names use a hyphen
e.g. J-N.Name-Name@ecmwf.int

ECMWF's public web site: http://www.ecmwf.int

	Ext
Director-General	
Dominique Marbouty	001
Deputy Director-General & Director of Operations	
Walter Zwieflhofer	003
Director of Research	
Erland Källén	005
Director of Administration	
Ute Dahremöller	007
Switchboard	
ECMWF switchboard	000
Advisory	
Internet mail addressed to Advisory@ecmwf.int	
Telefax (+44 118 986 9450, marked User Support)	
Computer Division	
Division Head	
Isabella Weger	050
Computer Operations Section Head	
Matthias Nethe	363
Networking and Computer Security Section Head	
Rémy Giraud	356
Servers and Desktops Section Head	
Duncan Potter	355
Systems Software Section Head	
Michael Hawkins	353
User Support Section Head	
Umberto Modigliani	382
User Support Staff	
Paul Dando	381
Dominique Lucas	386
Carsten Maaß	389
Pam Prior	384
Christian Weihrauch	380
Computer Operations	
Call Desk	303
Call Desk email: calldesk@ecmwf.int	
Console – Shift Leaders	803
Console fax number +44 118 949 9840	
Console email: newops@ecmwf.int	
Fault reporting – Call Desk	303
Registration – Call Desk	303
Service queries – Call Desk	303
Tape Requests – Tape Librarian	315

	Ext
Meteorological Division	
Division Head	
Erik Andersson	060
Data Services Group Leader	
Fabio Venuti	422
Meteorological Applications Section Head	
Alfred Hofstadler	400
Meteorological Data Section Head	
Baudouin Raoult	404
Meteorological Visualisation Section Head	
Stephan Siemen	375
Meteorological Operations Section Head	
David Richardson	420
Meteorological Analysts	
Antonio Garcia-Mendez	424
Anna Ghelli	425
Martin Janousek	460
Fernando Prates	421
Meteorological Operations Room	426
Data Division	
Division Head	
Jean-Noël Thépaut	030
Data Assimilation Section Head	
Lars Isaksen	852
Satellite Data Section Head	
Stephen English	660
Reanalysis Section Head	
Dick Dee	352
Predictability Division	
Division Head	
Roberto Buizza	653
Marine Aspects Section Head	
Peter Janssen	116
Probabilistic Forecasting Section Head	
Franco Molteni	108
Model Division	
Division Head	
Peter Bauer	080
Numerical Aspects Section Head	
Agathe Untch	704
Physical Aspects Section Head	
Anton Beljaars	035
GMES / MACC Coordinator	
Adrian Simmons	700
Education & Training (Acting)	
Sylvie Malardel	414
ECMWF library & documentation distribution	
Els Kooij-Connally	751